



**THE DATASHEET OF
PIC18F16Q40-I/SS**



PGA855 Low-Noise, Wide-Bandwidth, Fully Differential Output Programmable-Gain Instrumentation Amplifier

1 Features

- Eight pin-programmable binary gains
 - $G (V/V) = \frac{1}{8}, \frac{1}{4}, \frac{1}{2}, 1, 2, 4, 8,$ and 16
- Low gain error drift: 1 ppm/°C (max) at $G = 1 V/V$
- Fully differential outputs
 - Independent output power-supply pins to allow for ADC input overdrive protection
 - Output common-mode control
- Faster signal processing:
 - Wide bandwidth: 10 MHz at all gains
 - High slew rate: 35 V/μs
 - Settling time: 500 ns to 0.01%, 950 ns to 0.0015%
 - Input stage noise: 7.8 nV/√Hz at $G = 16 V/V$
 - Filter option to achieve better SNR
- Input overvoltage protection to ±40 V beyond supplies
- Input-stage supply range:
 - Single supply: 8 V to 36 V
 - Dual supply: ±4 V to ±18 V
- Output-stage supply range:
 - Single supply: 4.5 V to 36 V
 - Dual supply: ±2.25 V to ±18 V
- Specified temperature range: –40°C to +125°C
- Small package: 3-mm × 3-mm VQFN

2 Applications

- [Factory automation and control](#)
- [Analog input module](#)
- [Data acquisition \(DAQ\)](#)
- [Test and measurement](#)
- [Semiconductor test](#)

3 Description

The PGA855 is a high-bandwidth programmable gain instrumentation amplifier with fully differential outputs. The PGA855 is equipped with eight binary gain settings, from an attenuating gain of 0.125 V/V to a maximum of 16 V/V, using three digital gain selection pins. The output common-mode voltage can be independently set using the VOVM pin.

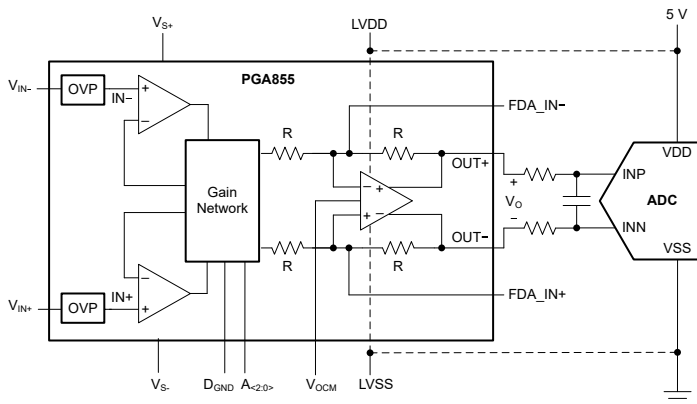
The PGA855 architecture is optimized to drive inputs of high-resolution, precision analog-to-digital converters (ADCs) with sampling rates up to 1 MSPS without the need for an additional ADC driver. The output-stage power supplies (LVSS/LVDD) are decoupled from the input stage and can be connected to power supplies of the ADC to protect the ADC or downstream device against overdrive damage.

The super-beta input transistors offer an impressively low input bias current, which in turn provides a very low input current noise density of 0.3 pA/√Hz, making the PGA855 a versatile choice for virtually any sensor type. The low-noise current-feedback front-end architecture offers excellent gain flatness, even at high frequencies, making the PGA855 an excellent high-impedance sensor readout device. Integrated protection circuitry on the input pins handles overvoltages up to ±40 V beyond the power-supply voltages.

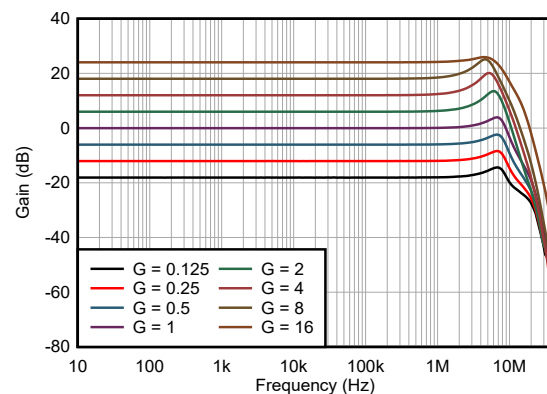
Package Information

PART NUMBER	PACKAGE ⁽¹⁾	PACKAGE SIZE ⁽²⁾
PGA855	RGT (VQFN, 16)	3 mm × 3 mm

- (1) For available packages, see the package option addendum.
- (2) The package size (length × width) is a nominal value and includes pins, where applicable.



PGA855 Simplified Application



Gain vs Frequency



Table of Contents

1 Features	1	8.4 Device Functional Modes.....	23
2 Applications	1	9 Application and Implementation	24
3 Description	1	9.1 Application Information.....	24
4 Revision History	2	9.2 Typical Applications.....	26
5 Device Comparison Table	3	9.3 Power Supply Recommendations.....	31
6 Pin Configuration and Functions	3	9.4 Layout.....	31
7 Specifications	4	10 Device and Documentation Support	33
7.1 Absolute Maximum Ratings.....	4	10.1 Device Support.....	33
7.2 ESD Ratings.....	4	10.2 Documentation Support.....	33
7.3 Recommended Operating Conditions.....	4	10.3 Receiving Notification of Documentation Updates..	33
7.4 Thermal Information.....	5	10.4 Support Resources.....	33
7.5 Electrical Characteristics.....	5	10.5 Trademarks.....	33
7.6 Typical Characteristics.....	8	10.6 Electrostatic Discharge Caution.....	33
8 Detailed Description	20	10.7 Glossary.....	33
8.1 Overview.....	20	11 Mechanical, Packaging, and Orderable Information	33
8.2 Functional Block Diagram.....	20		
8.3 Feature Description.....	21		

4 Revision History

NOTE: Page numbers for previous revisions may differ from page numbers in the current version.

Changes from Revision A (September 2023) to Revision B (September 2023)	Page
• Changed 4 MSPS to 1 MSPS in <i>Description</i> section.....	1
• Changed 4 MSPS to 1 MSPS in <i>Overview</i> section.....	20

Changes from Revision * (April 2023) to Revision A (September 2023)	Page
• Changed PGA855 status from advanced information (preview) to production data (active).....	1

5 Device Comparison Table

DEVICE	DESCRIPTION	GAIN EQUATION	RG PINS AT PIN
INA849	Ultra-low-noise (1-nV/√Hz), high-bandwidth instrumentation amplifier	$G = 1 + 6 \text{ k}\Omega / \text{RG}$	2, 3
INA851	Low-noise (3.2 nV/√Hz), high-speed (22 MHz), fully-differential instrumentation amp with overvoltage protection (±40 V)	$G = 1 + 6 \text{ k}\Omega / \text{RG}$	2, 3
PGA280	20-mV to ±10-V programmable gain instrumentation amplifier with 3-V or 5-V differential output; analog supply up to ±18 V	Digitally programmable with SPI	N/A
PGA281	Zero-drift, high-voltage programmable gain amplifier	Digitally pin-programmable	N/A

6 Pin Configuration and Functions

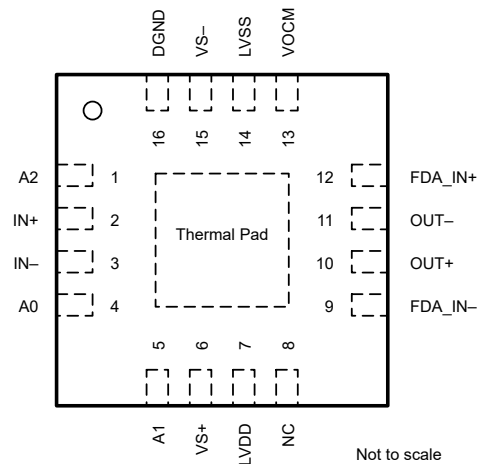


Figure 6-1. RGT Package, 16-Pin VQFN (Top View)

Table 6-1. Pin Functions

PIN		TYPE	DESCRIPTION
NAME	NO.		
A0	4	Input	Gain option pin 0
A1	5	Input	Gain option pin 1
A2	1	Input	Gain option pin 2
DGND	16	Power	Ground reference for digital logic and gain setting pins
FDA_IN-	9	Input	Connection to output driver summing node
FDA_IN+	12	Input	Connection to output driver summing node
IN-	3	Input	Negative (inverting) input
IN+	2	Input	Positive (noninverting) input
LVDD	7	Power	Output driver positive supply. Connect this pin to the positive supply of the ADC to protect from overdriving.
LVSS	14	Power	Output driver negative supply. Connect this pin to the negative supply of the ADC to protect from overdriving.
NC	8	—	Do not connect
OUT-	11	Output	Output (inverting)
OUT+	10	Output	Output (noninverting)
VOCM	13	Input	Level set for output common mode value
VS+	6	Power	Input stage positive supply
VS-	15	Power	Input stage negative supply
Thermal Pad	Thermal pad	—	The thermal pad must be soldered to the printed-circuit board (PCB). Connect thermal pad to a plane or large copper pour that is either floating or electrically connected to VS-, even for applications that have low power dissipation.

7 Specifications

7.1 Absolute Maximum Ratings

over operating free-air temperature range (unless otherwise noted)⁽¹⁾

		MIN	MAX	UNIT
V _S	Supply voltage on V _{S+} , V _{S-} pins; V _S = (V _{S+}) – (V _{S-})	0	40	V
V _{SOUT}	Supply voltage on LVDD, LVSS pins; V _{SOUT} = V _{LVDD} – V _{LVSS}	0	40	V
	Voltage on power pins LVDD, LVSS	(V _{S-}) – 0.5	(V _{S+}) + 0.5	V
V _{IN}	Voltage on signal-input pins IN+, IN–	(V _{S-}) – 40	(V _{S+}) + 40	V
	DGND, FDA_IN+, FDA_IN– pin voltage	(V _{S-}) – 0.5	(V _{S+}) + 0.5	V
	Voltage on gain-select pins A2, A1, A0	V _{DGND} – 0.5	(V _{S+}) + 0.5	V
V _O	Signal output pins maximum voltage on OUT+, OUT–	V _{LVSS} – 0.5	V _{LVDD} + 0.5	V
V _{OCM}	Output common-mode voltage	V _{LVSS} – 0.5	V _{LVDD} + 0.5	V
I _O	Signal-output pins current	–100	100	mA
I _{SC}	Output short-circuit current ⁽²⁾	Continuous		
T _A	Operating temperature	–50	150	°C
T _J	Junction Temperature		175	°C
T _{stg}	Storage Temperature	–65	150	°C

- (1) Operation outside the *Absolute Maximum Ratings* may cause permanent device damage. Absolute Maximum Ratings do not imply functional operation of the device at these or any other conditions beyond those listed under *Recommended Operating Conditions*. If used outside the *Recommended Operating Conditions* but within the *Absolute Maximum Ratings*, the device may not be fully functional, and this may affect device reliability, functionality, performance, and shorten the device lifetime.
- (2) Short-circuit to V_{SOUT} / 2.

7.2 ESD Ratings

			VALUE	UNIT
V _(ESD)	Electrostatic discharge	Human-body model (HBM), per ANSI/ESDA/JEDEC JS-001 ⁽¹⁾	±2000	V
		Charged-device model (CDM), per ANSI/ESDA/JEDEC JS-002 ⁽²⁾	±1000	

- (1) JEDEC document JEP155 states that 500-V HBM allows safe manufacturing with a standard ESD control process.
- (2) JEDEC document JEP157 states that 250-V CDM allows safe manufacturing with a standard ESD control process.

7.3 Recommended Operating Conditions

over operating free-air temperature range (unless otherwise noted)

			MIN	MAX	UNIT
V _S	Input stage supply voltage	Single supply	8	36	V
		Dual supply	±4	±18	
V _{SOUT}	Output stage supply voltage	Single supply	4.5	36	V
		Dual supply	±2.25	±18	
T _A	Specified temperature		–40	125	°C

7.4 Thermal Information

THERMAL METRIC ⁽¹⁾		PGA855	UNIT
		RGT (VQFN)	
		16 PINS	
R _{θJA}	Junction-to-ambient thermal resistance	47.3	°C/W
R _{θJC(top)}	Junction-to-case (top) thermal resistance	53.6	°C/W
R _{θJB}	Junction-to-board thermal resistance	22.0	°C/W
ψ _{JT}	Junction-to-top characterization parameter	1.4	°C/W
ψ _{JB}	Junction-to-board characterization parameter	22.0	°C/W
R _{θJC(bot)}	Junction-to-case (bottom) thermal resistance	7.8	°C/W

(1) For information about traditional and new thermal metrics, see the [Semiconductor and IC Package Thermal Metrics](#) application report.

7.5 Electrical Characteristics

at T_A = 25 °C, V_S = V_{SOUT} = ±15 V, V_{ICM} = V_{OCM} is at mid-supply, R_L = 10 kΩ, and G = 1 V/V (unless otherwise noted)

PARAMETER		TEST CONDITIONS		MIN	TYP	MAX	UNIT
INPUT							
V _{OS}	Differential offset voltage (input referred)	G = 1 to 16			±70	±350	μV
		G < 1			±70/G	±350/G	
	Differential offset voltage drift (input referred)	G = 1 to 16, T _A = -40°C to +125°C			±0.3	±1.0	μV/°C
		G < 1, T _A = -40°C to +125°C			±0.3/G	±1.0/G	
PSRR	Power-supply rejection ratio	±4 V ≤ V _S ≤ ±18 V, RTI	G = 0.125	102	108		dB
			G = 0.25	108	114		
			G = 0.5	114	120		
			G = 1	120	126		
			G = 2	120	126		
			G = 4	120	132		
			G = 8	120	136		
		G = 16	120	140			
Z _{id}	Differential impedance				100 1		GΩ pF
Z _{ic}	Common-mode impedance				100 7		GΩ pF
V _I	Input voltage	V _S = ±4 V to ±18 V, T _A = -40°C to +125°C		(V _{S-}) + 2.5		(V _{S+}) - 2.5	V
CMRR	Common-mode rejection ratio	At dc to 60 Hz, V _{ICM} = ±10 V, T _A = -40°C to +125°C, RTI	G = 0.125	64	82		dB
			G = 0.25	70	88		
			G = 0.5	76	94		
			G = 1	82	100		
			G = 2	88	106		
			G = 4	94	112		
			G = 8	100	118		
		G = 16	106	124			
BIAS CURRENT							
I _B	Input bias current				0.5	1.8	nA
		T _A = -40°C to +125°C			1		
	Input bias current drift	T _A = -40°C to +125°C				10	pA/°C
I _{OS}	Input offset current				0.5	1	nA
		T _A = -40°C to +125°C			1		
	Input offset current drift	T _A = -40°C to +125°C				10	pA/°C

7.5 Electrical Characteristics (continued)

at $T_A = 25\text{ }^\circ\text{C}$, $V_S = V_{SOUT} = \pm 15\text{ V}$, $V_{ICM} = V_{OCM}$ is at mid-supply, $R_L = 10\text{ k}\Omega$, and $G = 1\text{ V/V}$ (unless otherwise noted)

PARAMETER		TEST CONDITIONS		MIN	TYP	MAX	UNIT
NOISE VOLTAGE							
e_{NI}	Input-referred voltage noise density	$f = 1\text{ kHz}$	$G = 16$		7.8		nV/ $\sqrt{\text{Hz}}$
			$G = 8$		8.0		
			$G = 4$		8.6		
			$G = 2$		12.6		
			$G = 1$		21.6		
			$G = 0.5$		42		
			$G = 0.125$		168		
E_{NI}	Input-referred voltage noise	$f_B = 0.1\text{ Hz to }10\text{ Hz}$	$G = 16$		0.26		μV_{PP}
			$G = 8$		0.27		
			$G = 4$		0.29		
			$G = 2$		0.44		
			$G = 1$		0.8		
			$G = 0.5$		1.6		
			$G = 0.125$		6.4		
i_N	Input current noise density	$f = 1\text{ kHz}$			0.3		pA/ $\sqrt{\text{Hz}}$
I_N	Input current noise	$f_B = 0.1\text{ Hz to }10\text{ Hz}$			13		pA _{PP}
GAIN							
	Differential gain range			0.125		16	V/V
GE	Differential gain error	$G = 0.25, 0.5, 2, 4$			± 0.02	± 0.05	%
		$G = 1$			± 0.02	± 0.03	
		$G = 0.125, 8, 16$			± 0.03	± 0.07	
	Differential gain drift	$G = 1, T_A = -40\text{ }^\circ\text{C to }+125\text{ }^\circ\text{C}$				± 1	ppm/ $^\circ\text{C}$
		$G = 0.125, 0.25, 0.5, 2, 4, 8, 16, T_A = -40\text{ }^\circ\text{C to }+125\text{ }^\circ\text{C}$				± 2	
	Differential gain nonlinearity	$G = 0.125\text{ to }16, V_{OUTDIFF} = 10\text{ V}$	$T_A = -40\text{ }^\circ\text{C to }+125\text{ }^\circ\text{C}$		2	5	ppm
						10	
OUTPUT							
V_{OUT}	Output voltage	No load	$V_{SOUT} = \pm 2.25\text{ V}$	$V_{LVSS} + 0.1$		$V_{LVDD} - 0.1$	V
		$R_L = 10\text{ k}\Omega$	$V_{SOUT} = \pm 2.25\text{ V}$	$V_{LVSS} + 0.2$		$V_{LVDD} - 0.2$	
			$V_{SOUT} = \pm 18\text{ V}$	$V_{LVSS} + 0.4$		$V_{LVDD} - 0.4$	
C_L	Load capacitance	Stable operation for differential load			50		pF
I_{SC}	Short-circuit current	Continuous to $V_{SOUT} / 2$			± 45		mA
			$T_A = -40\text{ }^\circ\text{C to }+125\text{ }^\circ\text{C}$		± 20		
FREQUENCY RESPONSE							
BW	Bandwidth, -3 dB	$G = 0.125\text{ to }16$			10		MHz
SR	Slew rate	$G = 0.125\text{ to }16, V_{OUTDIFF} > 5\text{ V}$			35		V/ μs
t_S	Settling time	$G = 0.125\text{ to }16$ $V_{INDIFF} = 10\text{-V step}$ or $V_{OUTDIFF} = 10\text{-V step}$	To 0.01%		0.7		μs
			To 0.0015%		0.95		
	Gain switching time				2		μs
THD+N	Total harmonic distortion and Noise	Differential input, $f = 10\text{ kHz}, V_O = 10\text{ V}_{PP}$			-110		dB
		Single-ended input, $f = 10\text{ kHz}, V_O = 10\text{ V}_{PP}$			-105		
HD2	Second-order harmonic distortion	Differential input, $f = 10\text{ kHz}, V_O = 10\text{ V}_{PP}$			-120		dB
		Single-ended input, $f = 10\text{ kHz}, V_O = 10\text{ V}_{PP}$			-110		
HD3	Third-order harmonic distortion	Differential input, $f = 10\text{ kHz}, V_O = 10\text{ V}_{PP}$			-120		dB
		Single-ended input, $f = 10\text{ kHz}, V_O = 10\text{ V}_{PP}$			-110		

7.5 Electrical Characteristics (continued)

at $T_A = 25\text{ }^\circ\text{C}$, $V_S = V_{SOUT} = \pm 15\text{ V}$, $V_{ICM} = V_{OCM}$ is at mid-supply, $R_L = 10\text{ k}\Omega$, and $G = 1\text{ V/V}$ (unless otherwise noted)

PARAMETER		TEST CONDITIONS	MIN	TYP	MAX	UNIT
OUTPUT COMMON-MODE VOLTAGE (V_{OCM}) CONTROL						
V_{OCM}	Common-mode input voltage	$V_S = \pm 4\text{ V}$	$V_{LVSS} + 1.5$	$V_{LVDD} - 1.5$		V
		$V_S = \pm 18\text{ V}$	$V_{LVSS} + 2$	$V_{LVDD} - 2$		
	Small-signal bandwidth V_{OCM} pin	$V_{OCM} = 100\text{ mV}_{PP}$		16		MHz
	Large-signal bandwidth V_{OCM} pin	$V_{OCM} = 0.6\text{ V}_{PP}$		16		MHz
	DC output balance	V_{OCM} fixed at mid-supply ($V_O = \pm 1\text{ V}$)		70		dB
	Input impedance V_{OCM} pin			250 1		k Ω pF
	V_{OCM} offset from mid-supply	V_{OCM} pin floating		± 1	± 3.5	mV
	V_{OCM} offset voltage	$V_{OCM} = V_{ICM}$, $V_O = 0\text{ V}$		± 1	± 3.5	mV
	V_{OCM} offset voltage drift	$V_{OCM} = V_{ICM}$, $V_O = 0\text{ V}$, $T_A = -40\text{ }^\circ\text{C}$ to $+125\text{ }^\circ\text{C}$		± 20	± 40	$\mu\text{V}/\text{ }^\circ\text{C}$
INPUT STAGE POWER SUPPLY						
I_{Q_input}	Input stage quiescent current V_{S+} , V_{S-}	$V_{IN} = 0\text{ V}$		3	3.7	mA
		$T_A = -40\text{ }^\circ\text{C}$ to $+125\text{ }^\circ\text{C}$			4.5	
OUTPUT STAGE POWER SUPPLY						
I_{Q_output}	Output stage quiescent current V_{LVDD} , V_{LVSS}	$V_{IN} = 0\text{ V}$, V_{OCM} fixed at mid-supply		2.3	2.8	mA
		$T_A = -40\text{ }^\circ\text{C}$ to $125\text{ }^\circ\text{C}$			3.5	
DIGITAL LOGIC						
V_{IL}	Digital input logic low	A0, A1, A2 pins, referred to DGND	V_{DGND}	$V_{DGND} + 0.8$		V
V_{IH}	Digital input logic high	A0, A1, A2 pins, referred to DGND	$V_{DGND} + 1.8$		V_{S+}	V
	Digital input pin current	A0, A1, A2 pins		1.5	3	μA
V_{DGND}	DGND voltage		V_{S-}	$(V_{S+}) - 4$		V
	DGND reference current			4	10	μA

7.6 Typical Characteristics

at $T_A = 25^\circ\text{C}$, $V_S = V_{\text{SOUT}} = \pm 15\text{ V}$, $V_{\text{ICM}} = V_{\text{OCM}} = 0\text{ V}$, $R_L = 10\text{ k}\Omega$, and $G = 1\text{ V/V}$ (unless otherwise noted)

Table 7-1. Table of Graphs

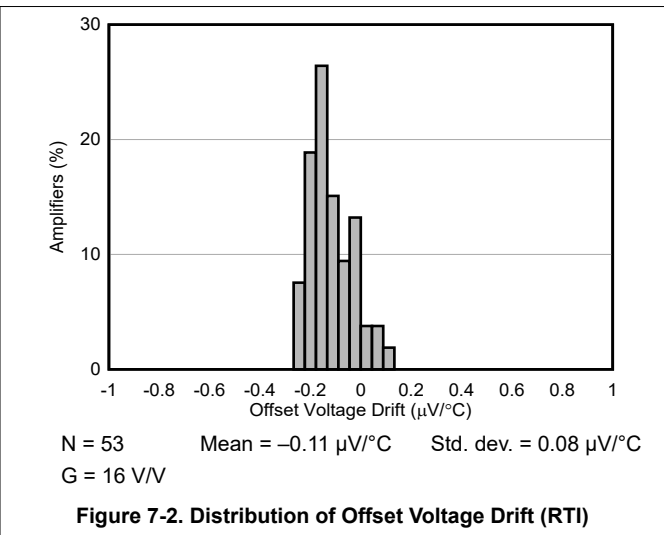
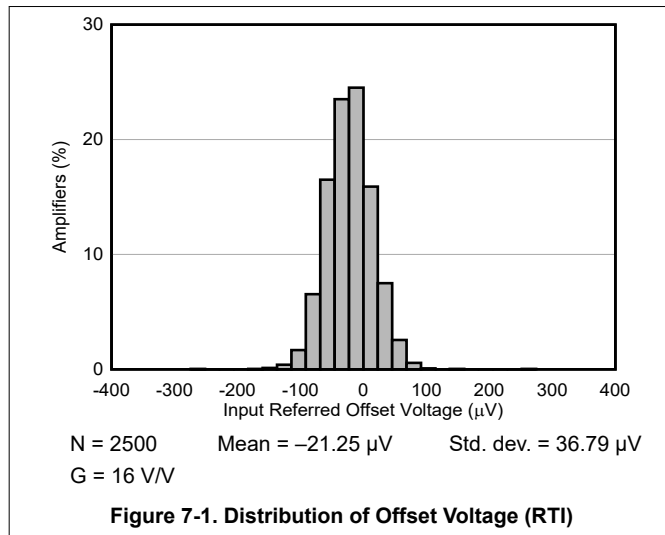
DESCRIPTION	FIGURE
Distribution of Offset Voltage (RTI), $G = 16\text{ V/V}$	Figure 7-1
Distribution of Offset Voltage Drift (RTI), $G = 16\text{ V/V}$	Figure 7-2
Distribution of Offset Voltage (RTI), $G = 1\text{ V/V}$	Figure 7-3
Distribution of Offset Voltage Drift (RTI), $G = 1\text{ V/V}$	Figure 7-4
Distribution of Offset Voltage (RTI), $G = 0.125\text{ V/V}$	Figure 7-5
Distribution of Offset Voltage Drift (RTI), $G = 0.125\text{ V/V}$	Figure 7-6
Distribution of Differential Gain Error, $G = 16\text{ V/V}$	Figure 7-7
Distribution of Differential Gain Error, $G = 1\text{ V/V}$	Figure 7-8
Gain Error vs Temperature, $G = 1\text{ V/V}$	Figure 7-9
Distribution of Differential Gain Error, $G = 0.125\text{ V/V}$	Figure 7-10
Distribution of Input Bias Current	Figure 7-11
Distribution of Input Bias Current, $T_A = 85^\circ\text{C}$	Figure 7-12
Input Bias Current vs Temperature	Figure 7-13
Input Bias Current vs Input Common-Mode Voltage	Figure 7-14
Distribution of Input Offset Current	Figure 7-15
Input Offset Current vs Temperature	Figure 7-16
Offset Voltage (RTI) vs Temperature, $G = 16\text{ V/V}$	Figure 7-17
Offset Voltage (RTI) vs Temperature	Figure 7-18
Offset Voltage (RTI) vs Temperature, $G = 0.125\text{ V/V}$	Figure 7-19
Offset Voltage (RTI) vs Input Common-Mode Voltage	Figure 7-20
CMRR Distribution, $G = 16\text{ V/V}$	Figure 7-21
CMRR Distribution, $G = 1\text{ V/V}$	Figure 7-22
CMRR Distribution, $G = 0.125\text{ V/V}$	Figure 7-23
CMRR vs Frequency (RTI)	Figure 7-24
CMRR vs Frequency (Unbalanced)	Figure 7-25
Typical CMRR vs Temperature	Figure 7-26
Positive PSRR vs Frequency	Figure 7-27
Negative PSRR vs Frequency	Figure 7-28
PSRR Distribution, $G = 16\text{ V/V}$	Figure 7-29
PSRR Distribution, $G = 1\text{ V/V}$	Figure 7-30
PSRR Distribution, $G = 0.125\text{ V/V}$	Figure 7-31
Gain Nonlinearity, $G = 16\text{ V/V}$	Figure 7-32
Gain Nonlinearity, $G = 1\text{ V/V}$	Figure 7-33
Gain Nonlinearity, $G = 0.125\text{ V/V}$	Figure 7-34
Voltage Noise Spectral Density (RTI) vs Frequency	Figure 7-35
0.1-Hz to 10-Hz Voltage Noise (RTI), $G = 16\text{ V/V}$	Figure 7-36
0.1-Hz to 10-Hz Voltage Noise (RTI), $G = 1\text{ V/V}$	Figure 7-37
0.1-Hz to 10-Hz Voltage Noise (RTI), $G = 0.125\text{ V/V}$	Figure 7-38
Current Noise Spectral Density vs Frequency	Figure 7-39
Gain vs Frequency	Figure 7-40
Large-Signal Step Response vs Frequency	Figure 7-41
Small-Signal Step Response, $G = 16\text{ V/V}$	Figure 7-42
Small-Signal Step Response, $G = 1\text{ V/V}$	Figure 7-43

7.6 Typical Characteristics

at $T_A = 25^\circ\text{C}$, $V_S = V_{SOUT} = \pm 15\text{ V}$, $V_{ICM} = V_{OCM} = 0\text{ V}$, $R_L = 10\text{ k}\Omega$, and $G = 1\text{ V/V}$ (unless otherwise noted)

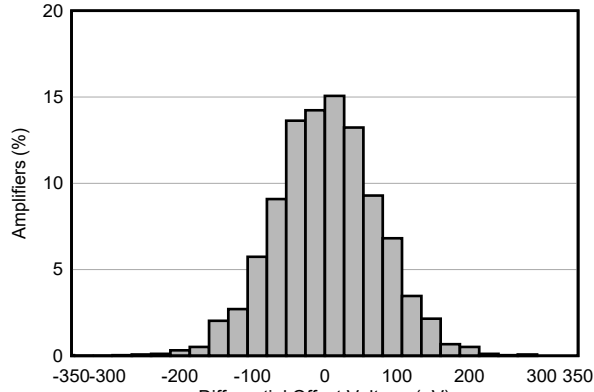
Table 7-1. Table of Graphs (continued)

DESCRIPTION	FIGURE
Small-Signal Step Response, $G = 0.125\text{ V/V}$	Figure 7-44
Large-Signal Step Response	Figure 7-45
Gain Switching Transient Response	Figure 7-46
Output Short-Circuit Current vs Temperature	Figure 7-47
Positive Output Voltage Swing vs Output Current	Figure 7-48
Negative Output Voltage Swing vs Output Current	Figure 7-49
Overload Recovery	Figure 7-50
Closed-Loop Output Impedance vs Frequency	Figure 7-51
Overshoot vs Capacitive Load	Figure 7-52
Quiescent Current vs Temperature	Figure 7-53
THD + Noise vs Frequency (22-kHz Filter)	Figure 7-54
THD + Noise vs Frequency (500-kHz Filter)	Figure 7-55
2nd Harmonic Distortion vs Frequency	Figure 7-56
3rd Harmonic Distortion vs Frequency	Figure 7-57
Total Harmonic Distortion vs Frequency vs Output Load	Figure 7-58
Ax Digital Input Pin Current vs Ax Digital Input Pin Voltage	Figure 7-59
DGND Digital Input Pin Current vs A2 Digital Input Pin Voltage	Figure 7-60
Digital Input Pin Current vs Temperature	Figure 7-61



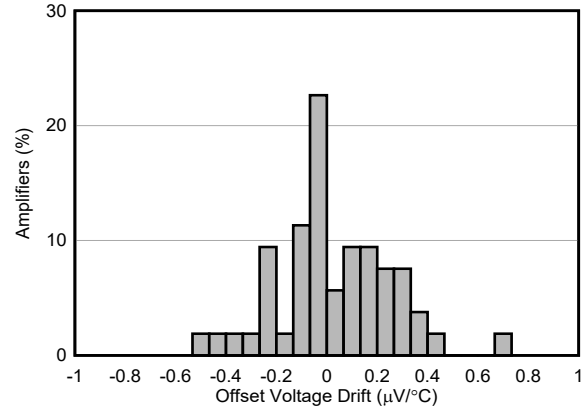
7.6 Typical Characteristics (continued)

at $T_A = 25^\circ\text{C}$, $V_S = V_{SOUT} = \pm 15\text{ V}$, $V_{ICM} = V_{OCM} = 0\text{ V}$, $R_L = 10\text{ k}\Omega$, and $G = 1\text{ V/V}$ (unless otherwise noted)



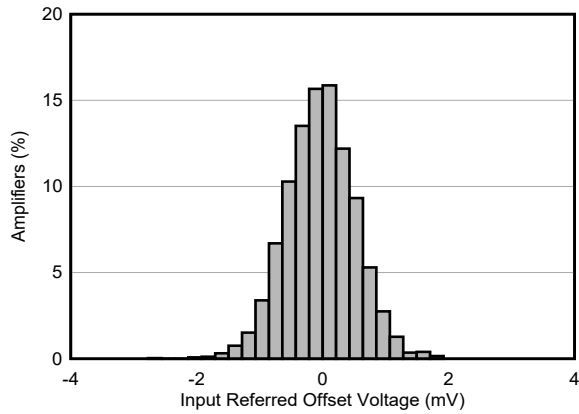
N = 2500 Mean = 2.83 μV Std. dev. = 71.58 μV
G = 1 V/V

Figure 7-3. Distribution of Offset Voltage (RTI)



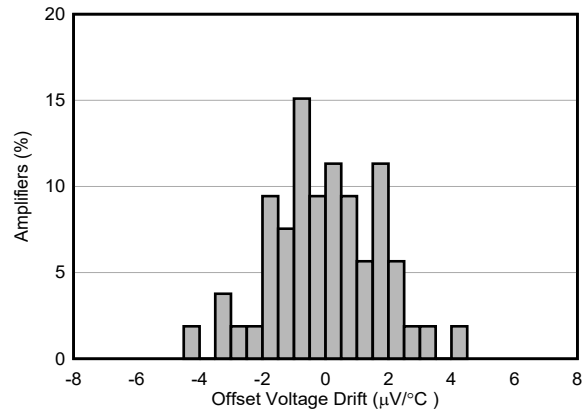
N = 53 Mean = -0.024 $\mu\text{V}/^\circ\text{C}$ Std. dev. = 0.22 $\mu\text{V}/^\circ\text{C}$
G = 1 V/V

Figure 7-4. Distribution of Offset Voltage Drift (RTI)



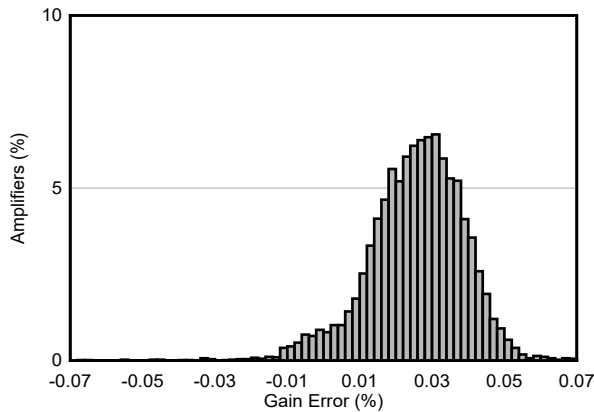
N = 2500 Mean = -36 μV Std. dev. = 540 μV
G = 0.125 V/V

Figure 7-5. Distribution of Offset Voltage (RTI)



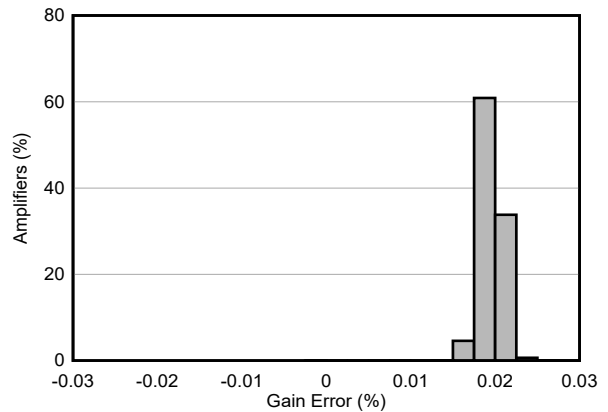
N = 53 Mean = -0.028 $\mu\text{V}/^\circ\text{C}$ Std. dev. = 1.69 $\mu\text{V}/^\circ\text{C}$
G = 0.125 V/V

Figure 7-6. Distribution of Offset Voltage Drift (RTI)



N = 7295 Mean = 0.0257 % Std. dev. = 0.0136 %
G = 16 V/V

Figure 7-7. Distribution of Differential Gain Error



N = 7295 Mean = 0.0195 % Std. dev. = 0.0012 %
G = 1 V/V

Figure 7-8. Distribution of Differential Gain Error

7.6 Typical Characteristics (continued)

at $T_A = 25^\circ\text{C}$, $V_S = V_{SOUT} = \pm 15\text{ V}$, $V_{ICM} = V_{OCM} = 0\text{ V}$, $R_L = 10\text{ k}\Omega$, and $G = 1\text{ V/V}$ (unless otherwise noted)

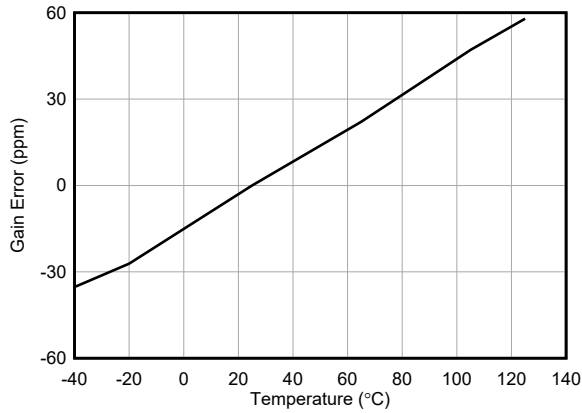


Figure 7-9. Gain Error vs Temperature

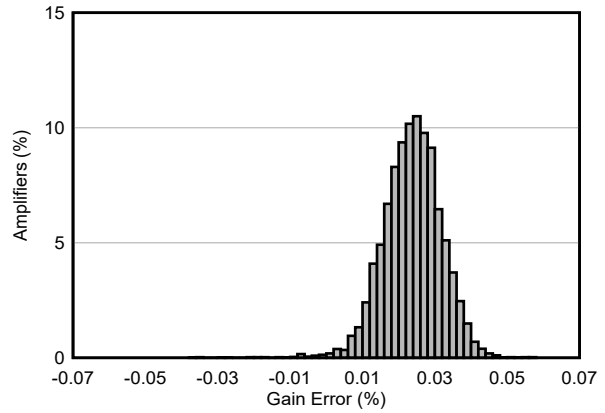


Figure 7-10. Distribution of Differential Gain Error

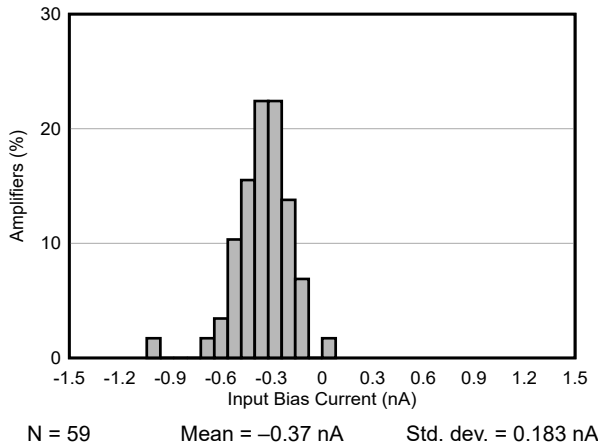


Figure 7-11. Distribution of Input Bias Current

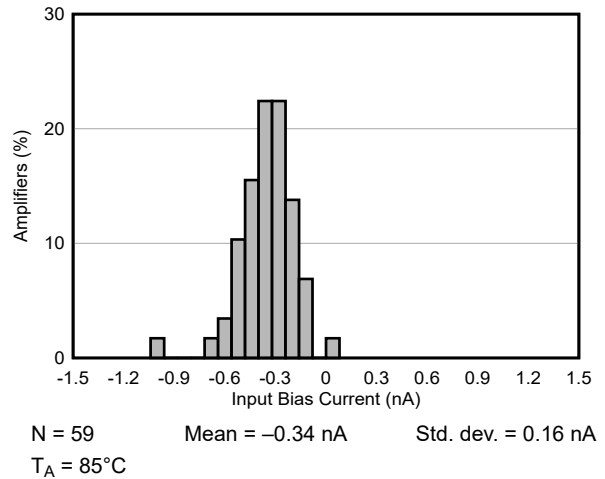


Figure 7-12. Distribution of Input Bias Current

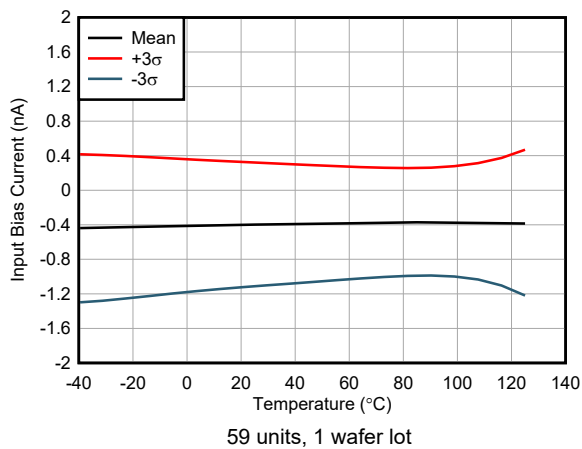


Figure 7-13. Input Bias Current vs Temperature

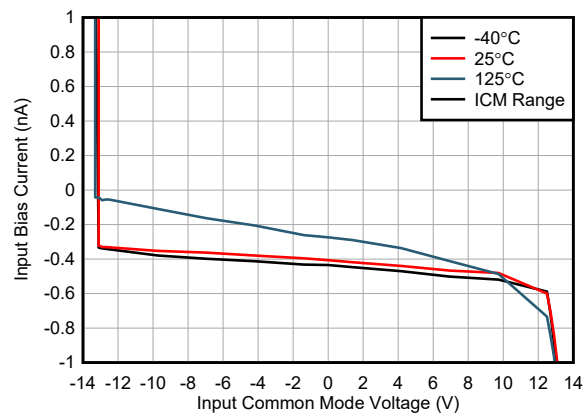


Figure 7-14. Input Bias Current vs Input Common-Mode Voltage

7.6 Typical Characteristics (continued)

at $T_A = 25^\circ\text{C}$, $V_S = V_{SOUT} = \pm 15\text{ V}$, $V_{ICM} = V_{OCM} = 0\text{ V}$, $R_L = 10\text{ k}\Omega$, and $G = 1\text{ V/V}$ (unless otherwise noted)

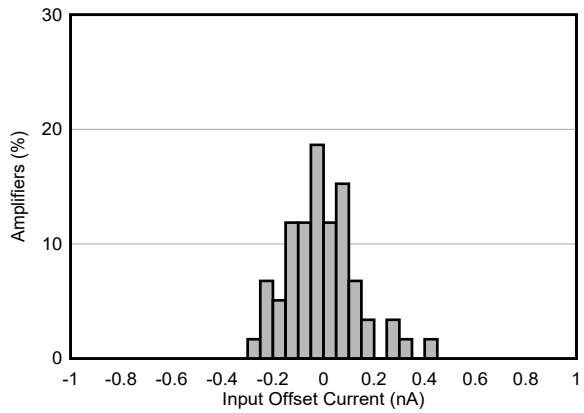


Figure 7-15. Distribution of Input Offset Current

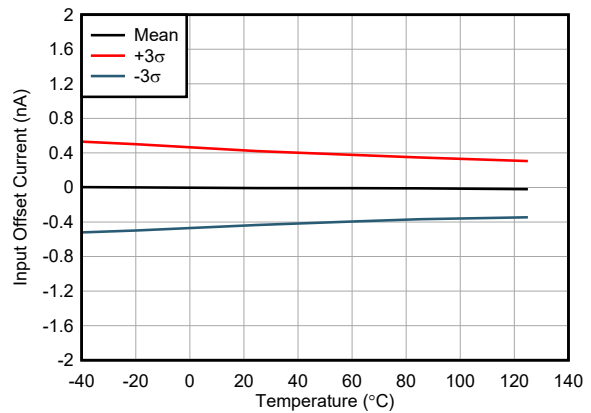


Figure 7-16. Input Offset Current vs Temperature

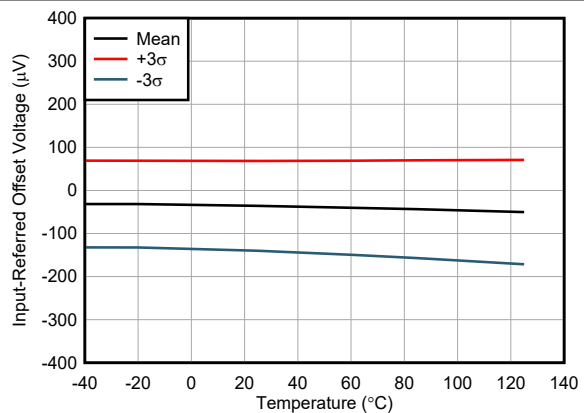


Figure 7-17. Offset Voltage (RTI) vs Temperature

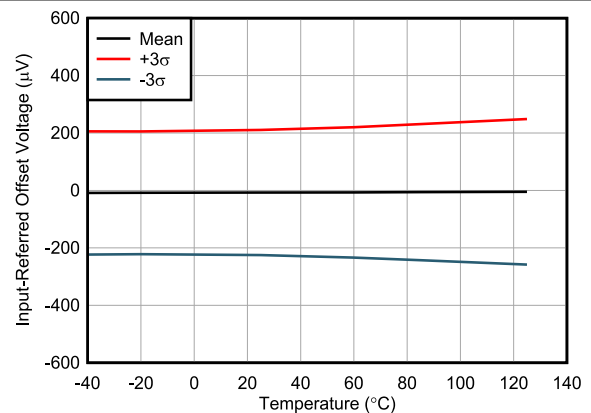


Figure 7-18. Offset Voltage (RTI) vs Temperature

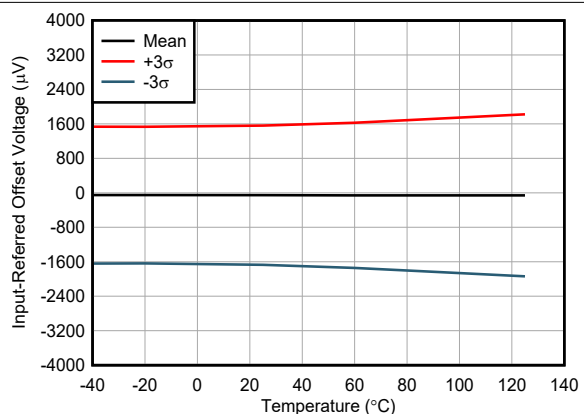


Figure 7-19. Offset Voltage (RTI) vs Temperature

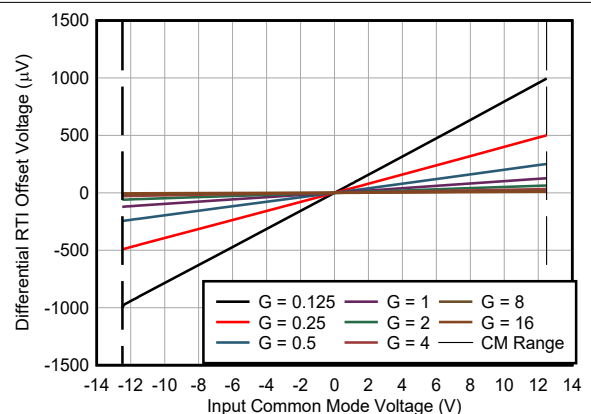


Figure 7-20. Offset Voltage (RTI) vs Input Common-Mode Voltage

7.6 Typical Characteristics (continued)

at $T_A = 25^\circ\text{C}$, $V_S = V_{SOUT} = \pm 15\text{ V}$, $V_{ICM} = V_{OCM} = 0\text{ V}$, $R_L = 10\text{ k}\Omega$, and $G = 1\text{ V/V}$ (unless otherwise noted)

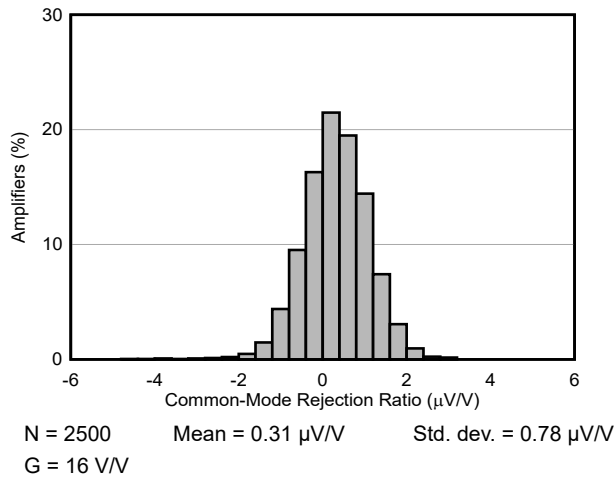


Figure 7-21. CMRR Distribution

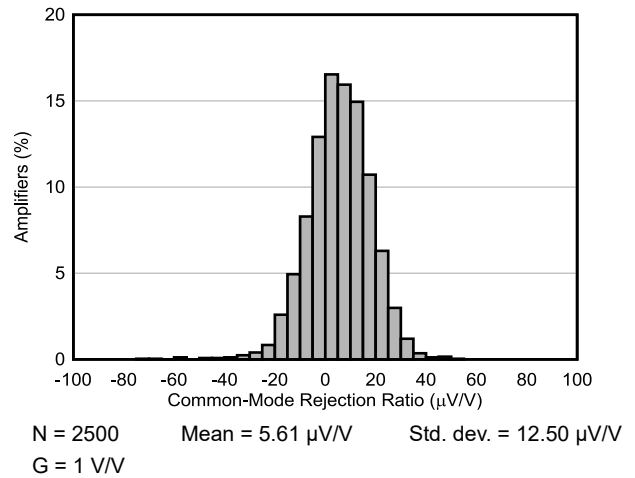


Figure 7-22. CMRR Distribution

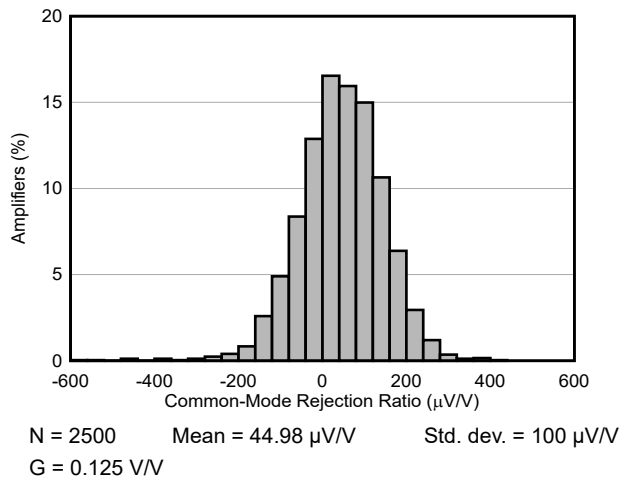


Figure 7-23. CMRR Distribution

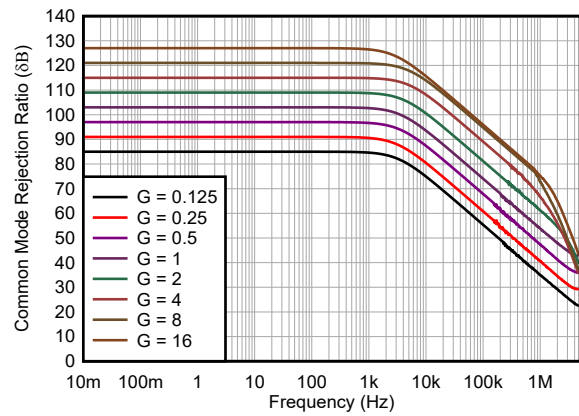


Figure 7-24. CMRR vs Frequency (RTI)

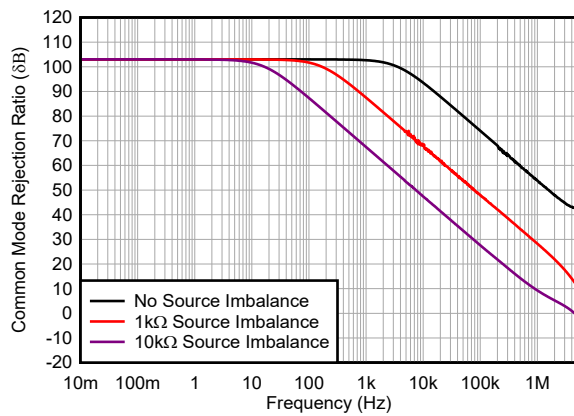


Figure 7-25. CMRR vs Frequency (Unbalanced)

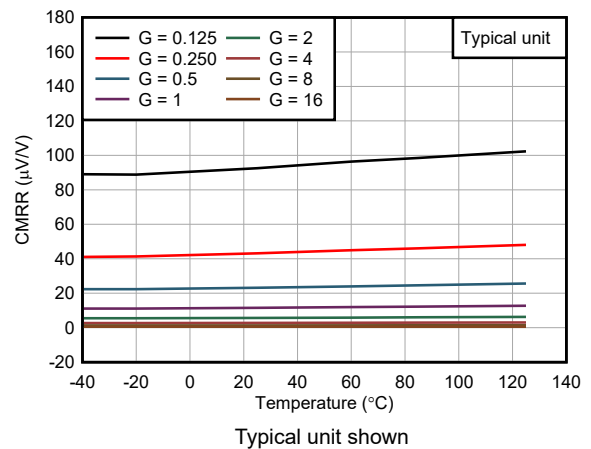


Figure 7-26. Typical CMRR vs Temperature

7.6 Typical Characteristics (continued)

at $T_A = 25^\circ\text{C}$, $V_S = V_{SOUT} = \pm 15\text{ V}$, $V_{ICM} = V_{OCM} = 0\text{ V}$, $R_L = 10\text{ k}\Omega$, and $G = 1\text{ V/V}$ (unless otherwise noted)

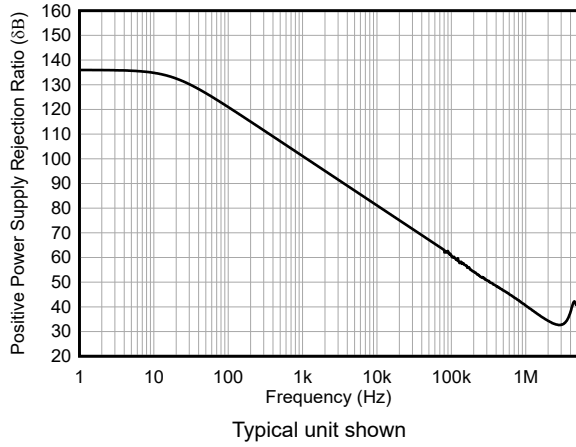


Figure 7-27. Positive PSRR vs Frequency

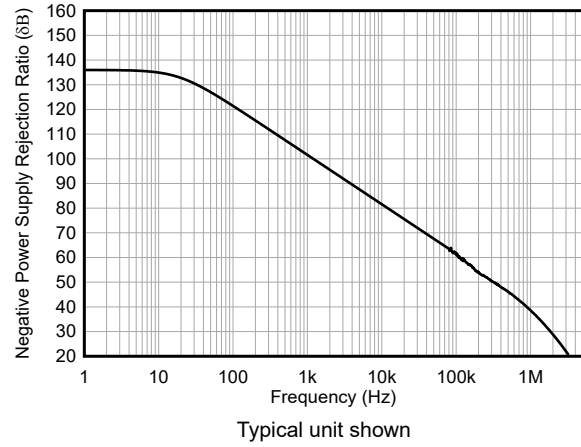


Figure 7-28. Negative PSRR vs Frequency

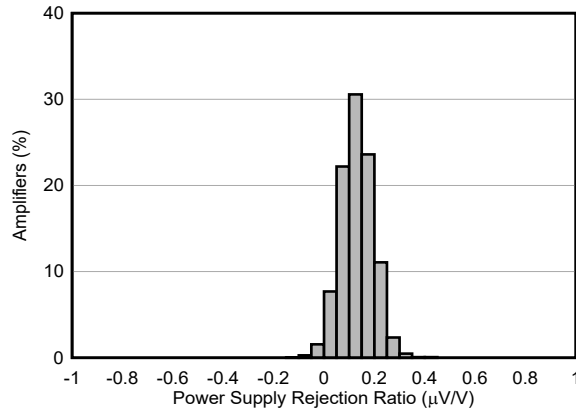


Figure 7-29. PSRR Distribution

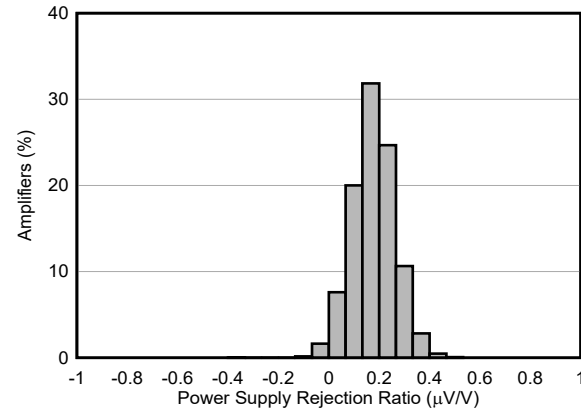


Figure 7-30. PSRR Distribution

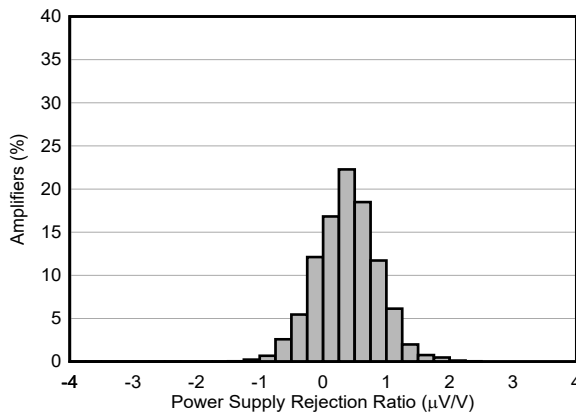


Figure 7-31. PSRR Distribution

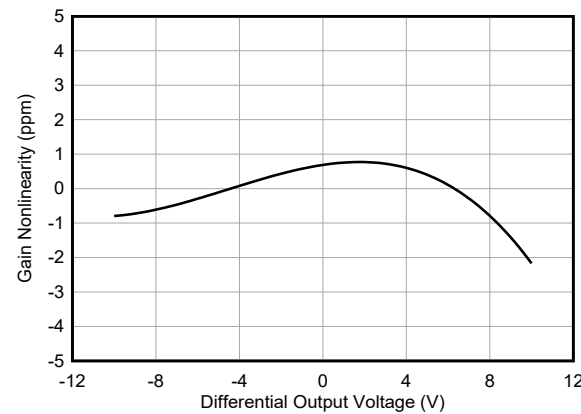


Figure 7-32. Gain Nonlinearity

7.6 Typical Characteristics (continued)

at $T_A = 25^\circ\text{C}$, $V_S = V_{SOUT} = \pm 15\text{ V}$, $V_{ICM} = V_{OCM} = 0\text{ V}$, $R_L = 10\text{ k}\Omega$, and $G = 1\text{ V/V}$ (unless otherwise noted)

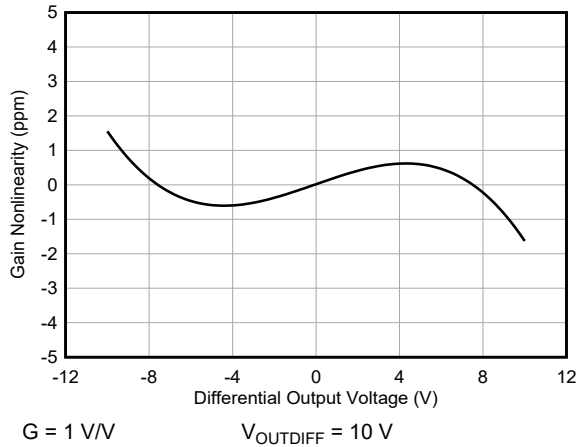


Figure 7-33. Gain Nonlinearity

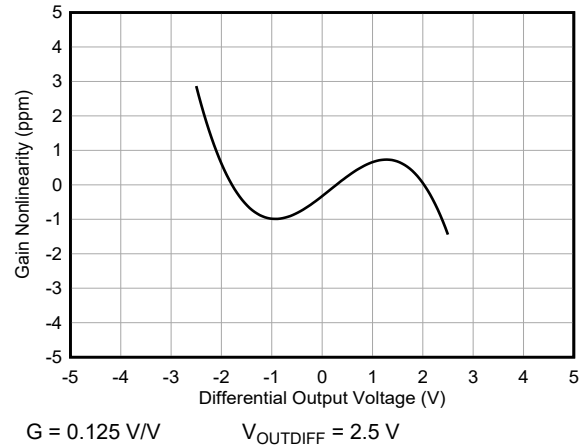


Figure 7-34. Gain Nonlinearity

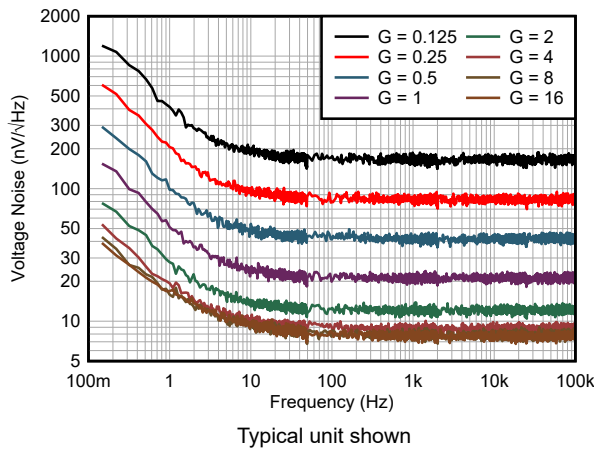


Figure 7-35. Voltage Noise Spectral Density (RTI) vs Frequency

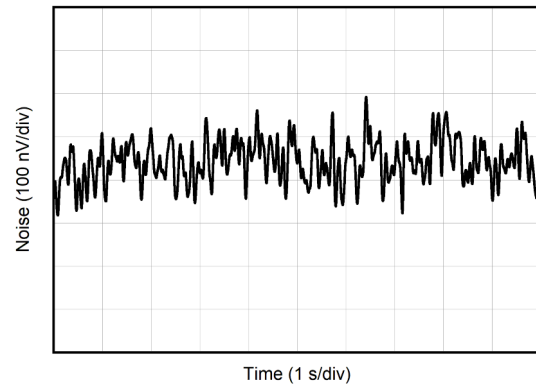


Figure 7-36. 0.1-Hz to 10-Hz Voltage Noise (RTI)

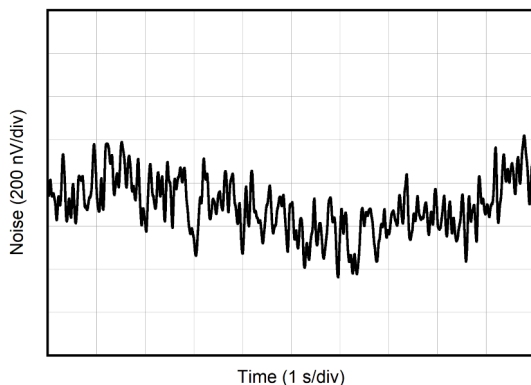


Figure 7-37. 0.1-Hz to 10-Hz Voltage Noise (RTI)

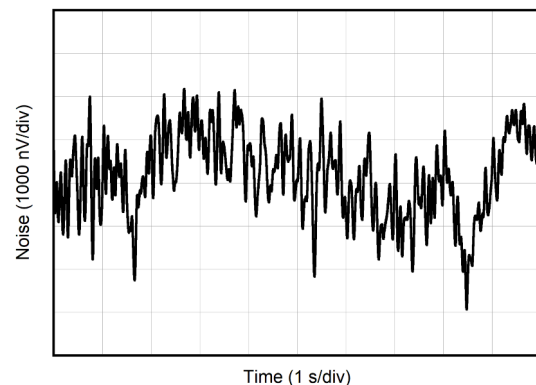
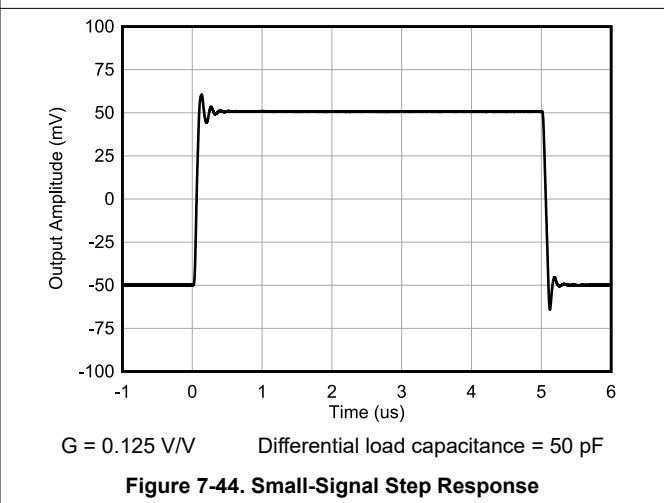
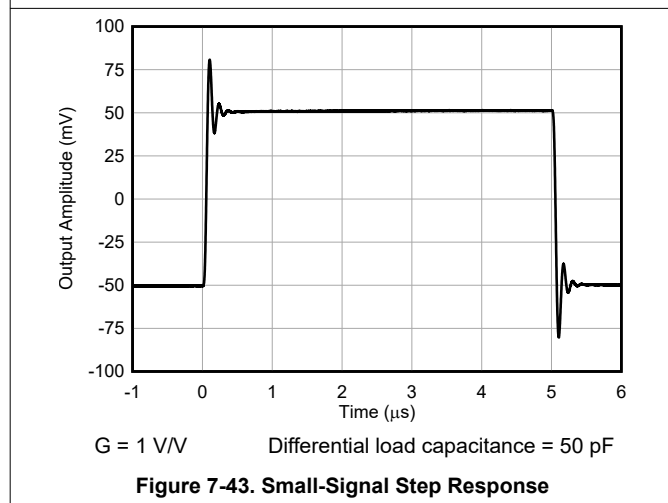
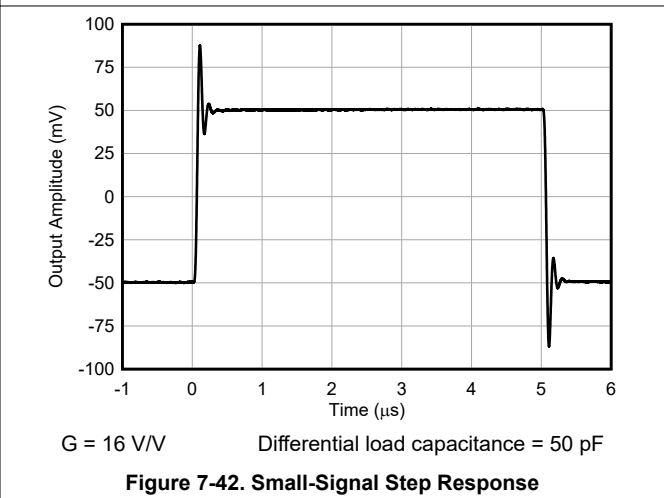
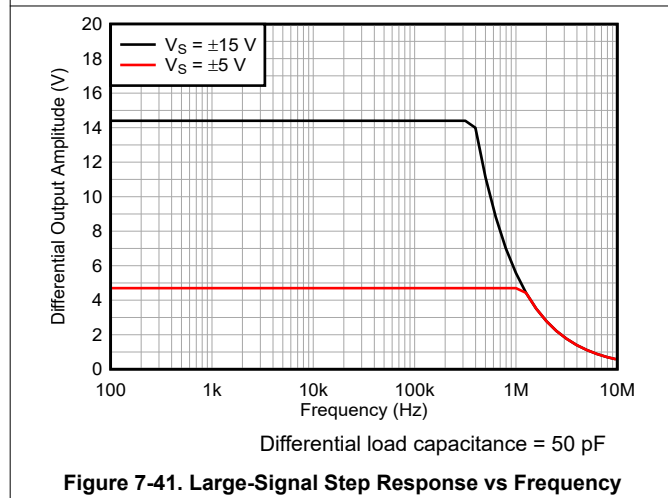
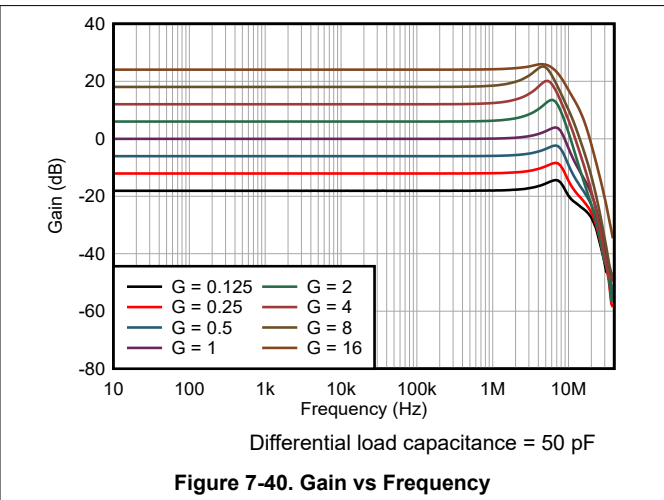
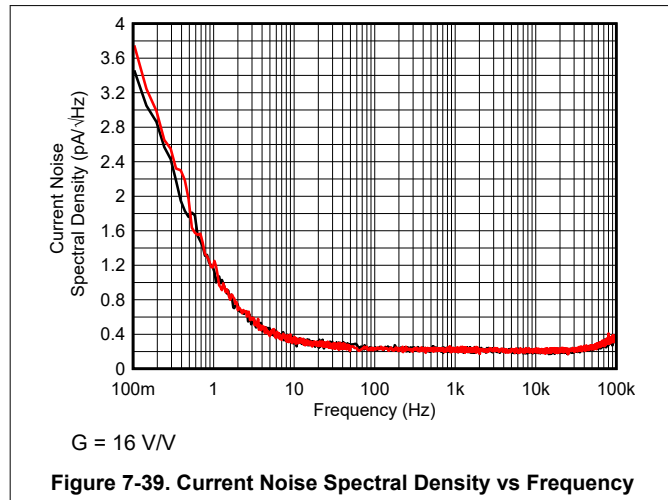


Figure 7-38. 0.1-Hz to 10-Hz Voltage Noise (RTI)

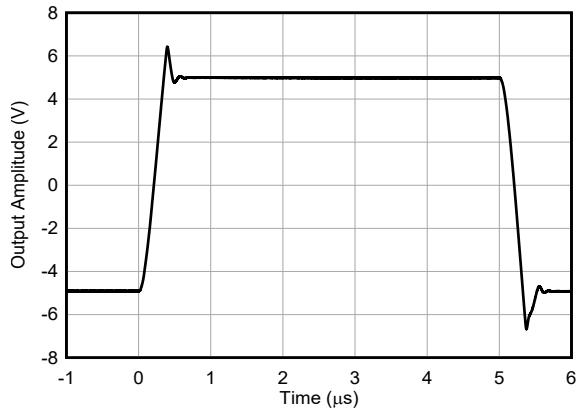
7.6 Typical Characteristics (continued)

at $T_A = 25^\circ\text{C}$, $V_S = V_{SOUT} = \pm 15\text{ V}$, $V_{ICM} = V_{OCM} = 0\text{ V}$, $R_L = 10\text{ k}\Omega$, and $G = 1\text{ V/V}$ (unless otherwise noted)



7.6 Typical Characteristics (continued)

at $T_A = 25^\circ\text{C}$, $V_S = V_{SOUT} = \pm 15\text{ V}$, $V_{ICM} = V_{OCM} = 0\text{ V}$, $R_L = 10\text{ k}\Omega$, and $G = 1\text{ V/V}$ (unless otherwise noted)



$G = 1\text{ V/V}$

Figure 7-45. Large-Signal Step Response

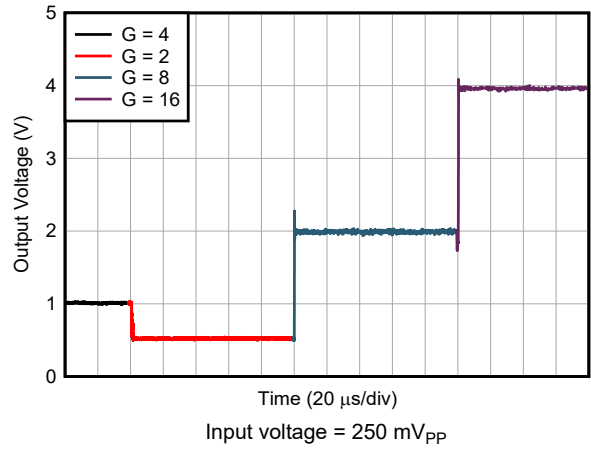


Figure 7-46. Gain Switching Transient Response

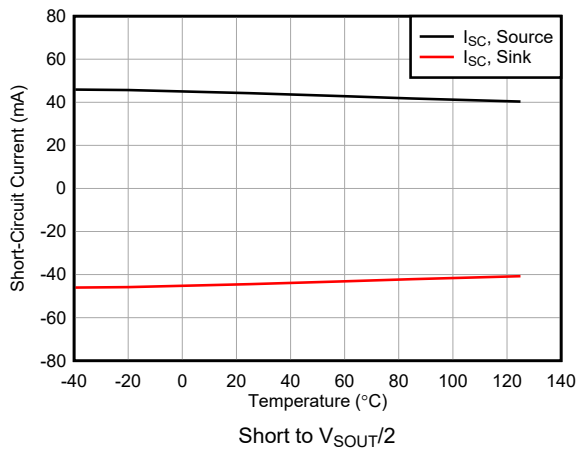
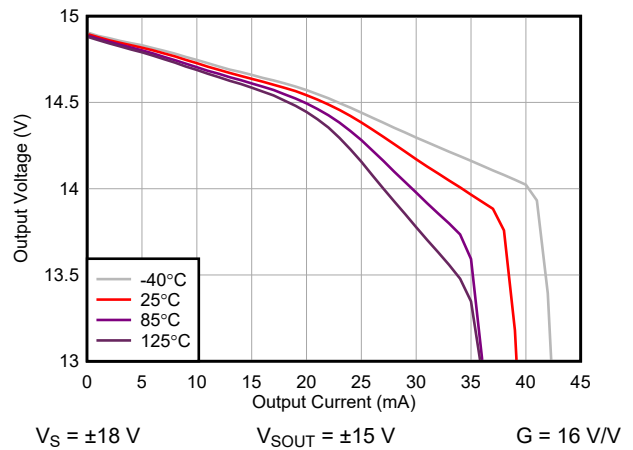
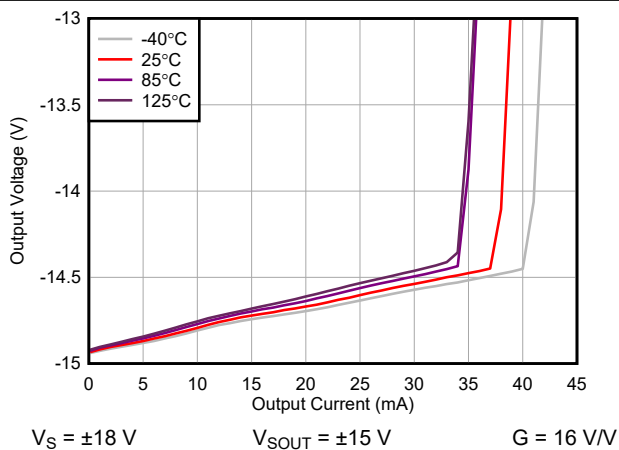


Figure 7-47. Output Short-Circuit Current vs Temperature



$V_S = \pm 18\text{ V}$ $V_{SOUT} = \pm 15\text{ V}$ $G = 16\text{ V/V}$

Figure 7-48. Positive Output Voltage vs Output Current



$V_S = \pm 18\text{ V}$ $V_{SOUT} = \pm 15\text{ V}$ $G = 16\text{ V/V}$

Figure 7-49. Negative Output Voltage vs Output Current

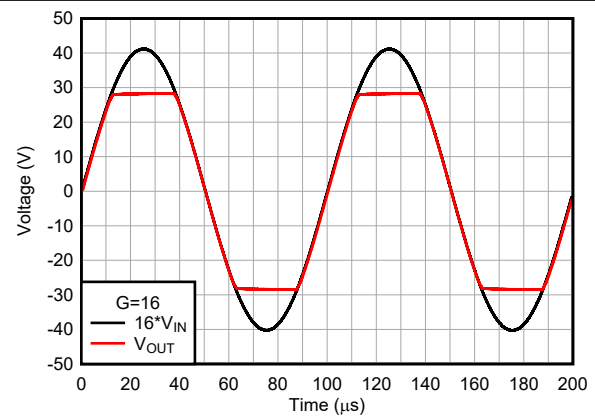


Figure 7-50. Overload Recovery

7.6 Typical Characteristics (continued)

at $T_A = 25^\circ\text{C}$, $V_S = V_{SOUT} = \pm 15\text{ V}$, $V_{ICM} = V_{OCM} = 0\text{ V}$, $R_L = 10\text{ k}\Omega$, and $G = 1\text{ V/V}$ (unless otherwise noted)

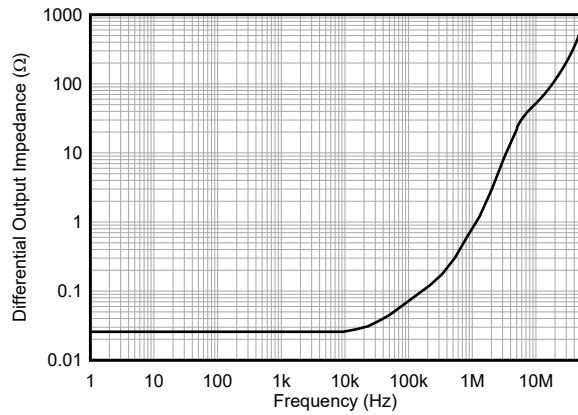


Figure 7-51. Closed Loop Output Impedance vs Frequency

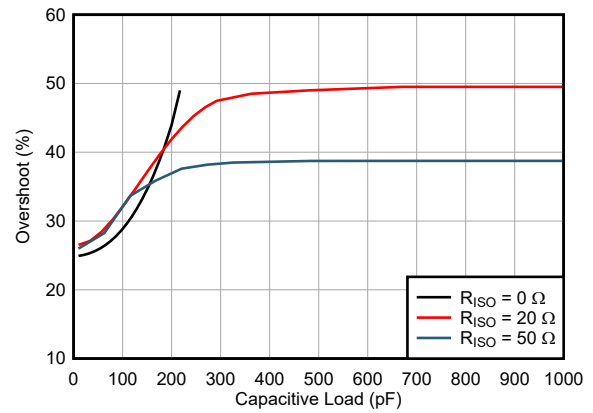


Figure 7-52. Overshoot vs Capacitive Load

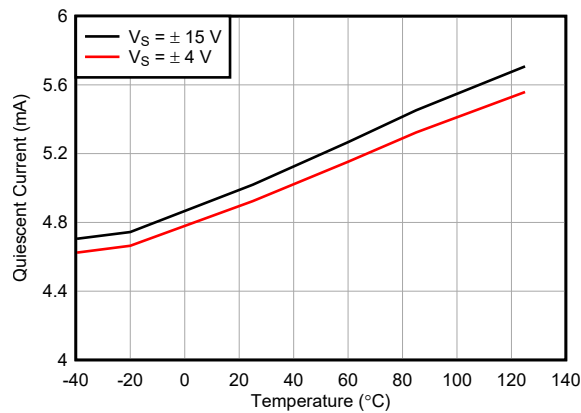
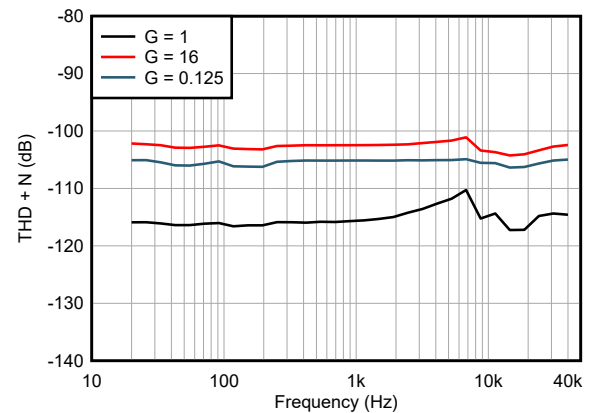
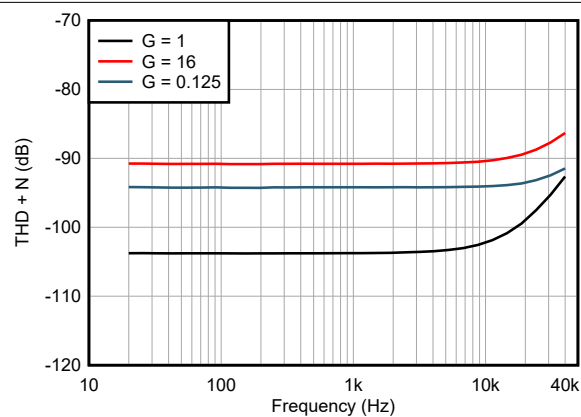


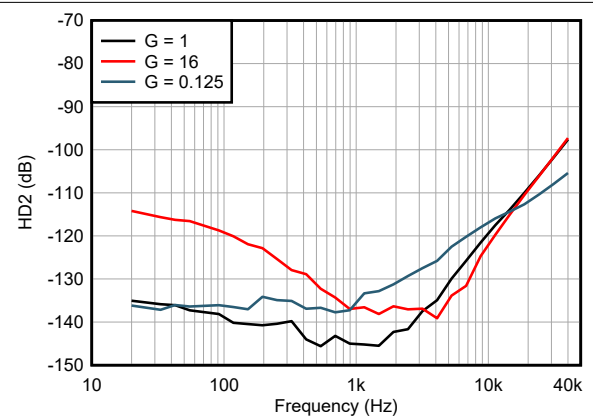
Figure 7-53. Quiescent Current vs Temperature



10-Hz to 22-kHz band-pass filter $V_{OUTDIFF} > 2.5\text{ V}_{PP}$
Figure 7-54. Total Harmonic Distortion + Noise vs Frequency



10-Hz to 500-kHz band-pass filter $V_{OUTDIFF} > 2.5\text{ V}_{PP}$
Figure 7-55. Total Harmonic Distortion + Noise vs Frequency



$V_{OUTDIFF} > 2.5\text{ V}_{PP}$
Figure 7-56. 2nd Harmonic Distortion vs Frequency

7.6 Typical Characteristics (continued)

at $T_A = 25^\circ\text{C}$, $V_S = V_{SOUT} = \pm 15\text{ V}$, $V_{ICM} = V_{OCM} = 0\text{ V}$, $R_L = 10\text{ k}\Omega$, and $G = 1\text{ V/V}$ (unless otherwise noted)

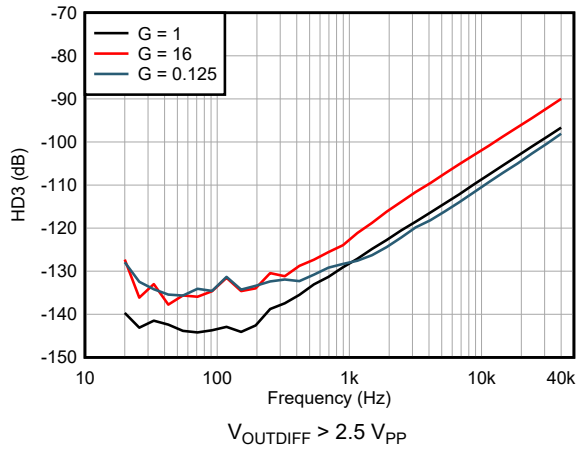


Figure 7-57. 3rd Harmonic Distortion vs Frequency

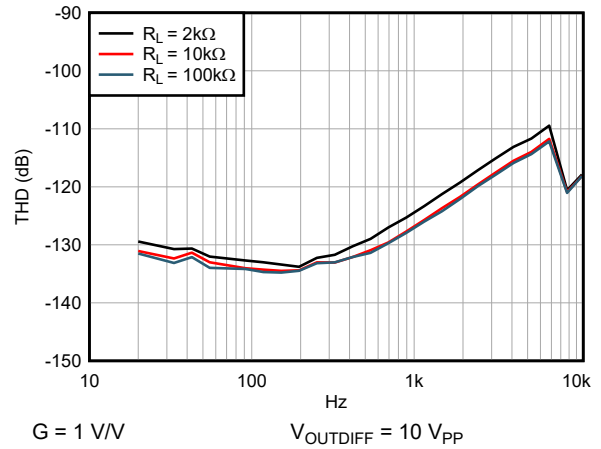


Figure 7-58. Total Harmonic Distortion vs Frequency

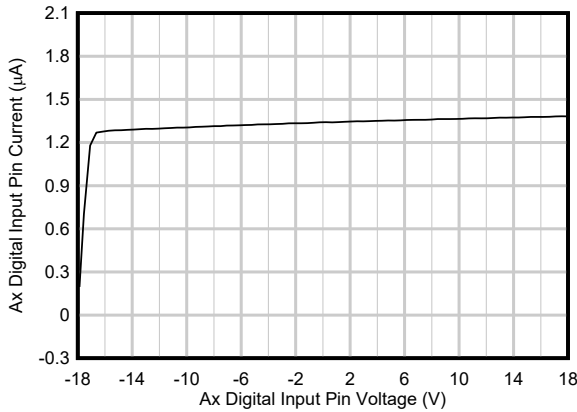


Figure 7-59. Ax Digital Input Pin Current vs Ax Digital Input Pin Voltage

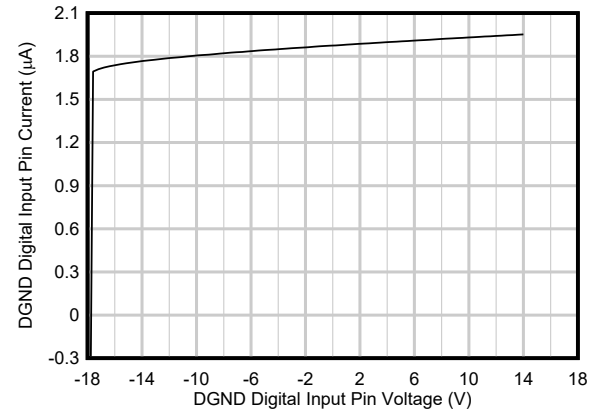


Figure 7-60. DGND Digital Input Pin Current vs DGND Digital Input Pin Voltage

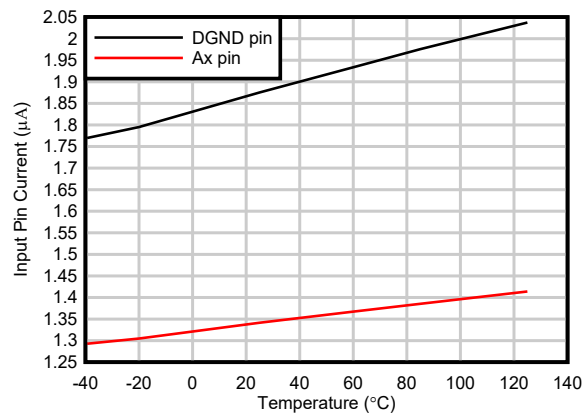


Figure 7-61. Digital Input Pin Current vs Temperature

8 Detailed Description

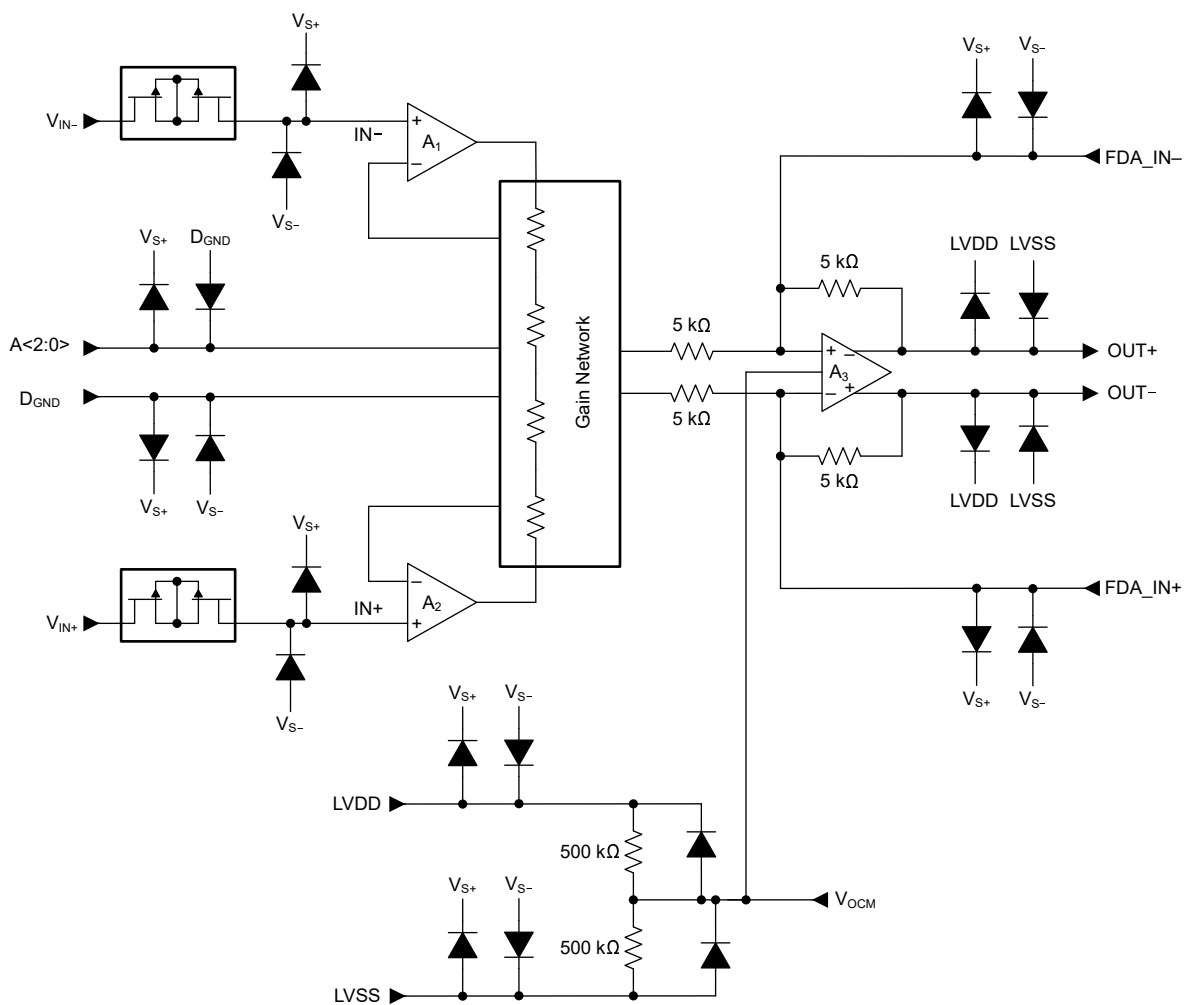
8.1 Overview

The PGA855 is a monolithic, high-voltage, precision programmable-gain instrumentation amplifier. The PGA855 combines a high-speed current-feedback input stage with an internally matched gain resistor network, followed by a four-resistor, fully differential amplifier output stage. Eight preprogrammed binary gains, ranging from 0.125 V/V to 16 V/V are selectable using gain-select pins A0, A1, and A2.

A functional block diagram for PGA855 is shown in the next section. The differential input voltage is fed into a pair of matched, high-impedance input-current-feedback amplifiers. An integrated precision-matched gain resistor network is used to amplify the differential input voltage. A fully differential output difference amplifier, A₃, rejects the input common-mode component and refers the output signal to the voltage level set by the V_{OCM} pin.

The PGA855 output amplifier bandwidth is optimized to drive high-performance analog-to-digital converters (ADCs) with sampling rates up to 1 MSPS without the need for an additional ADC driver. The output amplifier uses a separate power supply that is independent of the input-stage power supply. When driving an ADC, use a low-impedance connection from LVDD and LVSS to the ADC power supplies. This configuration protects the ADC inputs from damage due to inadvertent overvoltage conditions.

8.2 Functional Block Diagram



8.3 Feature Description

8.3.1 Gain Control

The PGA855 uses three pins to set the amplifier gain. These gain select pins are set with respect to DGND. This configuration simplifies design when compared to programmable-gain amplifiers requiring an SPI or other digital interface options for gain changes. Figure 8-1 shows the gain-setting block diagram. Table 8-1 lists the gain options. Any gain select pin that is not driven by an external source is automatically biased at DGND using internal pulldown options.

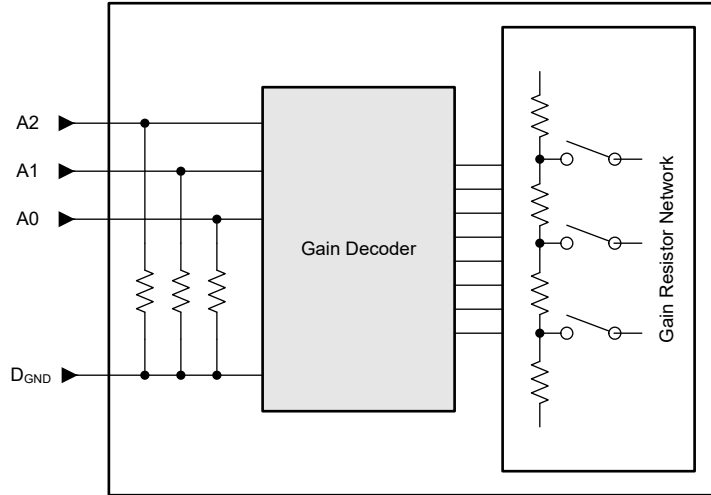


Figure 8-1. PGA855 Gain Setting Block Diagram

Table 8-1. Gain Options

A2:A0	GAIN
000	0.125
001	0.25
010	0.5
011	1
100	2
101	4
110	8
111	16

8.3.2 Input Protection

The inputs of PGA855 are individually protected for voltages up to ± 40 V beyond either supply. For example, an input common-mode voltage anywhere between -55 V and $+55$ V does not cause damage when powered from ± 15 -V supplies. Internal circuitry on each input provides low series impedance under normal signal conditions, thus maintaining high performance under normal operating conditions. If the input is overloaded, the protection circuitry limits the input current to a value of approximately 4.8 mA. Figure 8-2 shows the input protection functionality during an overvoltage condition.

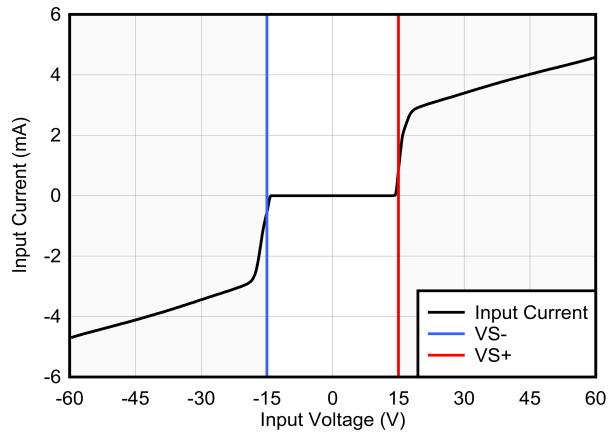


Figure 8-2. Input Current vs Input Overvoltage

Figure 8-3 shows that during an input overvoltage condition, current flows through the input protection diodes into the power supplies. In applications where the power supplies are unable to sink current, place Zener diode clamps (ZD1 and ZD2) on the power supplies to provide a current pathway to ground.

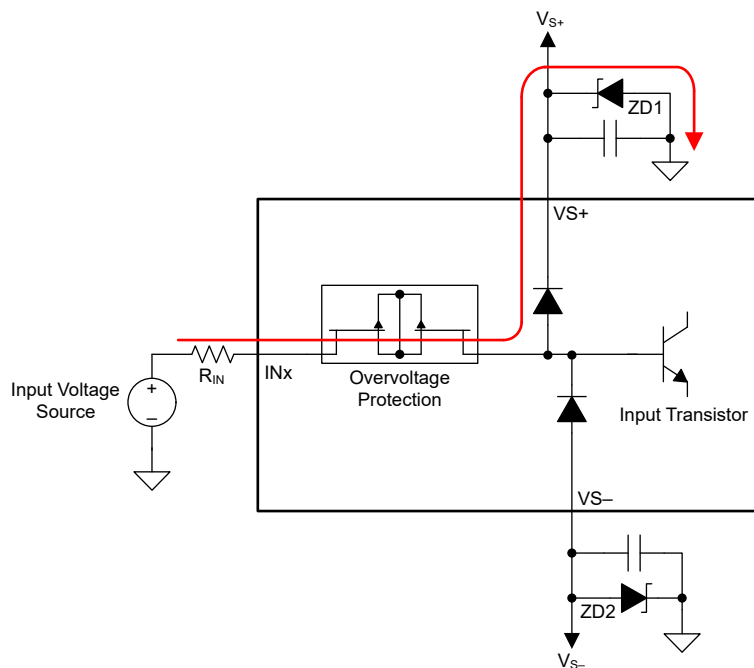


Figure 8-3. Input Current Path During an Overvoltage Condition

8.3.3 Output Common-Mode Pin

The output voltages of the PGA855 are balanced with respect to the voltage on the output common-mode pin, VO_{CM}. The starting point for most designs is to assign an output common-mode voltage for the PGA855. For ac-coupled signal paths, this voltage is often the default mid-supply voltage, so as to retain the most available output swing around the voltage centered at VO_{CM}. For dc-coupled signal paths, set this voltage between a maximum of $V_{LVDD} - 1.5\text{ V}$ and minimum of $V_{LVSS} + 1.5\text{ V}$. For precision ADC applications, this voltage is typically the input common-mode voltage of the ADC.

The voltage at the VO_{CM} pin is internally buffered to bias the fully differential output amplifier, eliminating the need for an external VO_{CM} buffer. In the event that the VO_{CM} pin is left floating, the output common-mode voltage is biased at output mid-supply using an internal 500-k Ω / 500-k Ω resistor divider network connected between the output-stage power-supply pins.

8.3.4 Using the Fully Differential Output Amplifier to Shape Noise

Section 8.2 shows that the PGA855 output-stage fully-differential amplifier uses 5-k Ω feedback resistors between the OUT+ and OUT– outputs and the inverting and noninverting inputs, respectively. External direct access to the inverting and noninverting inputs of the fully differential amplifier is provided through the FDA_IN– and FDA_IN+ pins, respectively. This option allows circuit designers to add external feedback capacitors in parallel with the internal feedback resistors to implement noise-filtering or noise-shaping techniques. These pins can also be used to implement customized attenuating gains for the output stage. Consider the following important factors when designing parallel circuits with the internal feedback resistors:

- The accuracy of the internal resistor network is 0.01 % or better. This accuracy results in a common-mode rejection (CMRR) of 80 dB or better. Mismatched leakage currents on these pins can cause CMRR degradation.
- The internal resistors have $\pm 15\%$ absolute resistance variation and must be considered when implementing custom attenuating gains or noise filters.

CAUTION

Do not treat these pins as outputs, nor use the pins to source or sink current. Excessive currents through the feedback resistors can cause permanent damage to internal circuitry.

8.4 Device Functional Modes

The PGA855 has a single functional mode and operates when the input-stage power supply is greater than $\pm 4\text{ V}$ (8 V) and the output-stage power supply is greater than $\pm 2.25\text{ V}$ (4.5 V); see also Section 7.3.

9 Application and Implementation

Note

Information in the following applications sections is not part of the TI component specification, and TI does not warrant its accuracy or completeness. TI's customers are responsible for determining suitability of components for their purposes, as well as validating and testing their design implementation to confirm system functionality.

9.1 Application Information

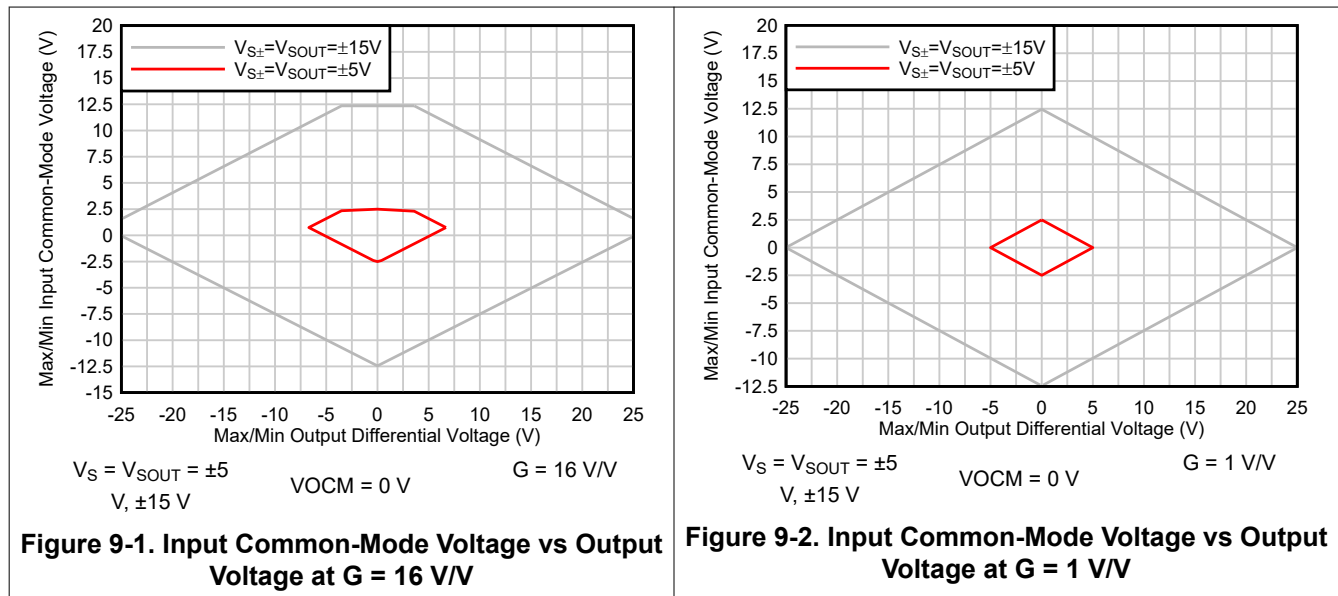
The PGA855 is a monolithic, high-voltage, high bandwidth, precision programmable gain instrumentation amplifier with fully differential outputs. The PGA855 combines a high-speed current-feedback input stage with an internally matched gain resistor network, followed by a four-resistor, fully differential amplifier output stage. The PGA855 is equipped with 8 binary-gain settings, from 0.125 V/V to 16 V/V, using three digital gain-selection pins: A0, A1, and A2.

The PGA855 is designed to work with applications such as factory automation and control, analog input modules, data acquisition, test and measurement, and semiconductor test.

9.1.1 Linear Operating Input Range

The linear operating input voltage range of the PGA855 input circuitry extends within 2.5 V (maximum) of both power supplies, and maintains excellent common-mode rejection throughout this range. The linear operating input common-mode range is a function of the input common-mode voltage, input differential voltage, gain, and output common-mode voltage.

The valid common-mode range to enable valid output voltage at no load condition are shown in Figure 9-1 to Figure 9-3.



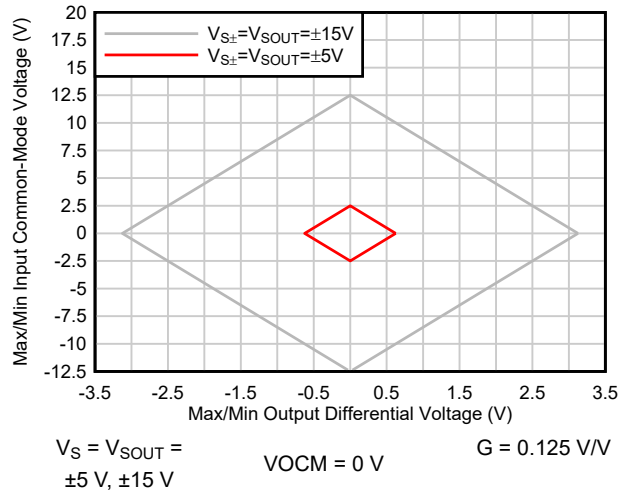


Figure 9-3. Input Common-Mode Voltage vs Output Voltage at $G = 0.125 \text{ V/V}$

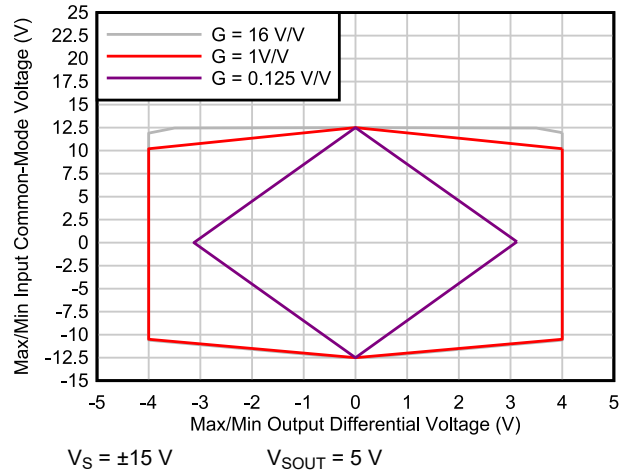


Figure 9-4. Input Common-Mode Voltage vs Output Voltage at $\text{VO}_{\text{CM}} = 2.5 \text{ V}$

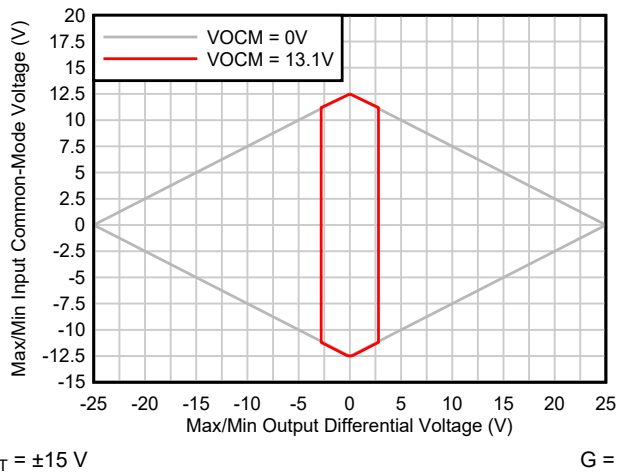


Figure 9-5. Input Common-Mode Voltage vs Output Voltage at $\text{VO}_{\text{CM}} \text{ max}$

9.2 Typical Applications

9.2.1 ADS127L11 and ADS127L21, 24-Bit, Delta-Sigma ADC Driver Circuit

The application circuit in [Figure 9-6](#) shows a schematic for a 24-bit wide-bandwidth, delta-sigma ADC. The [ADS127Lx1](#) ADC offers two digital filters to optimize ac applications (wideband filter) or dc applications (sinc4 filter). [Table 9-2](#) and [Table 9-3](#) show measurement results in both filter settings. For a detailed design procedure to operate the [ADS127Lx1](#) ADC, see the [ADS127Lx1EVM-PDK evaluation module user's guide](#).

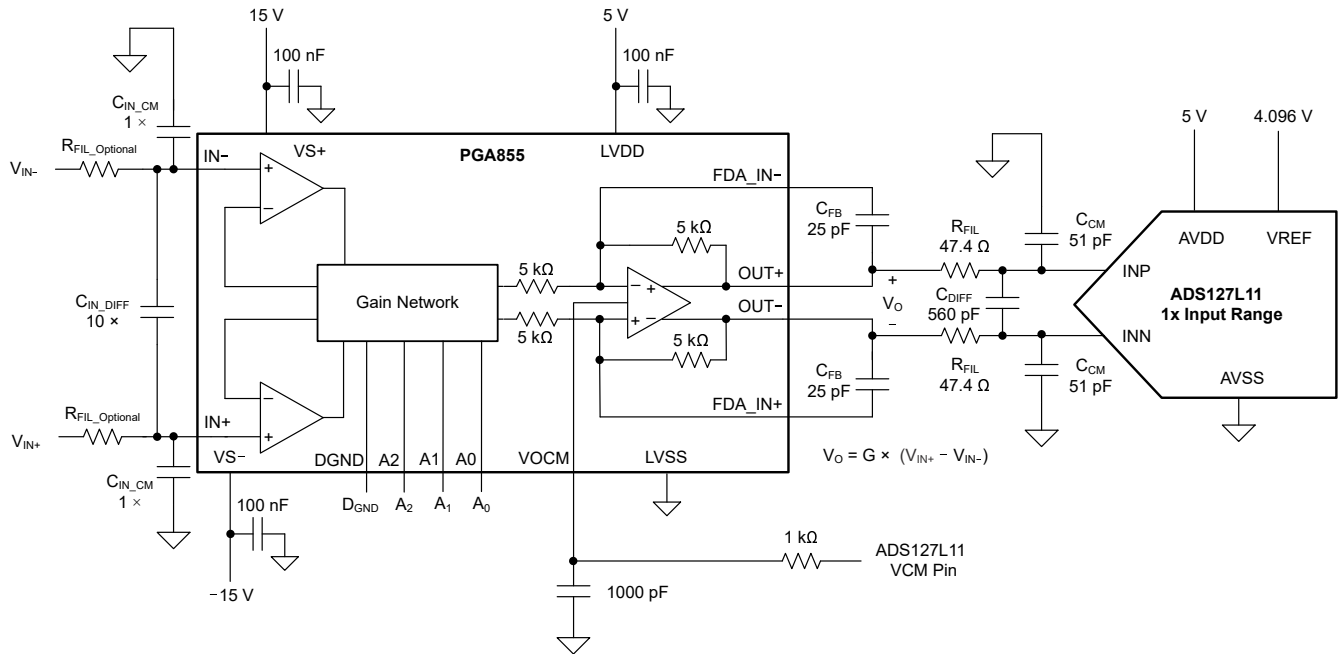


Figure 9-6. Driving the ADS127Lx1 Delta-Sigma ADC

9.2.1.1 Design Requirements

The design requirements for the application driving the [ADS127Lx1](#) ADC are listed in the following table.

Table 9-1. Design Parameters

PARAMETER	VALUE
Differential-to-differential conversion	V_{INDIFF} to $V_{OUTDIFF}$
Supply voltages	$V_{S\pm} = \pm 15\text{ V}$, $V_{LVDD} = 5\text{ V}$, $V_{LVSS} = \text{GND}$, $V_{REF} = 4.096\text{ V}$
Full-scale range of ADC	$\text{FSR} = \pm 4.096\text{ V}$
Data rate of ADC	$f_{\text{DATA}} = 187.5\text{ kSPS}$
ADC filter configuration	(1) High-speed mode, Sinc4 filter, $\text{OSR} = 64$ (2) High-speed mode, Wideband filter, $\text{OSR} = 64$
PGA gain	See Table 9-2 and Table 9-3
Signal frequency	Tested at $f_{\text{IN}} = 1\text{ kHz}$
RC kickback filter ⁽¹⁾	$R_{\text{FIL}} = 47.4\ \Omega$, $C_{\text{DIFF}} = 560\text{ pF}$, $C_{\text{CM}} = 51\text{ pF}$

- (1) Consider a trade-off between THD, frequency response, and drift. The differential current drift into the ADC can interact with the filter resistors and result in higher drift errors. However, lower resistance degrades the phase margin of the PGA855. For low drift applications, keep $R_{\text{FIL}} < 50\ \Omega$.

9.2.1.2 Detailed Design Procedure

Table 9-2 and Table 9-3 show the typical signal-to-noise (SNR) and total harmonic distortion (THD) of the PGA855 driving the ADS127Lx1 delta-sigma ADC using a sinc4 or wideband filter. Figure 9-7 and Figure 9-8 show the respective FFT plots. For the SNR and THD measurements, a 1-kHz differential signal is applied. The signal amplitude is adjusted to produce a PGA855 output at -0.2 dBFS of the ADC full-scale range. For a list of the equivalent input voltage amplitude signals for the different PGA855 gain configurations, see Table 9-2 and Table 9-3. At gain = 1 V/V, the design achieves -121.4 -dB THD and 109.1-dB SNR.

Table 9-2. PGA855 and ADS127Lx1 FFT Data Summary, OSR = 64, Sinc4 Filter

PGA GAIN (V/V)	INPUT AMPLITUDE (V _{PP})	SNR (dB)	THD (dB)	ENOB (Bits)
0.125	40.0	106.0	-119.6	17.5
0.25	32.022	109.0	-119.3	17.8
0.5	16.012	109.8	-121.2	17.9
1	8.006	109.6	-121.4	17.9
2	4.002	109.6	-121.4	17.9
4	2.002	107.4	-121.4	17.5
8	1.0	104.0	-121.4	17.0
16	0.5	99.1	-117.0	16.2

Table 9-3. PGA855 and ADS127Lx1 FFT Data Summary, OSR = 64, Wideband Filter

PGA GAIN (V/V)	INPUT AMPLITUDE (V _{PP})	SNR (dB)	THD (dB)	ENOB (Bits)
0.125	40.0	106.0	-119.6	17.3
0.25	32.022	107.5	-119.0	17.5
0.5	16.012	107.7	-121.2	17.6
1	8.006	107.6	-121.4	17.6
2	4.002	107.0	-121.4	17.5
4	2.002	105.4	-121.4	17.2
8	1.0	101.7	-121.4	16.6
16	0.5	96.7	-117.0	15.8

The R-C-R differential low-pass filter at the input of the instrumentation amplifier helps reduce EMI/RFI high-frequency extrinsic noise. This filter can be customized per the bandwidth and application requirements. This design example (see [Figure 9-6](#)) suggests a filter with the capacitor ratio of $C_{IN_DIFF} = 10 \times C_{IN_CM}$. Using the 10-to-1 ratio for differential capacitor C_{IN_DIFF} versus common-mode capacitors C_{IN_CM} offers good differential and common-mode noise rejection, and this arrangement tends to be less sensitive to the tolerance variation and mismatch of the filter capacitors.

The feedback capacitor, C_{FB} , is in parallel with the PGA855 output-stage 5-k Ω feedback resistors to implement additional noise filtering. The internal resistors have $\pm 15\%$ absolute resistance variation, and this variation must be taken in to account when implementing noise filtering. In this example, C_{FB} is set to 25 pF, providing a typical f_{-3dB} corner frequency of 1 MHz. The estimated minimum f_{-3dB} corner frequency for this circuit is approximately 938 kHz when accounting for the feedback-resistor variation.

The filter at the ADS127Lx1 inputs works as a charge reservoir to filter the sampled input of the ADC. The charge reservoir reduces the instantaneous charge demand of the amplifier, maintaining low distortion and low gain error that otherwise can degrade because of incomplete amplifier settling. The ADC input filter values are $R_{FIL} = 47.4\ \Omega$, $C_{DIFF} = 560\ \text{pF}$, and $C_{CM} = 51\ \text{pF}$. The ADC input precharge buffers significantly reduce the sample-phase input charge that raises the ADC input impedance to decrease gain error.

High-grade COG (NPO) are used everywhere in the signal path (C_{IN_DIFF} , C_{IN_CM} , C_{FB} , C_{DIFF} , C_{CM}) for low distortion. Among ceramic surface-mount capacitors, COG (NPO) ceramic capacitors provide the best capacitance accuracy. The type of dielectric used in COG (NPO) ceramic capacitors provides the most stable electrical properties over voltage, frequency, and temperature changes.

9.2.1.3 Application Curves

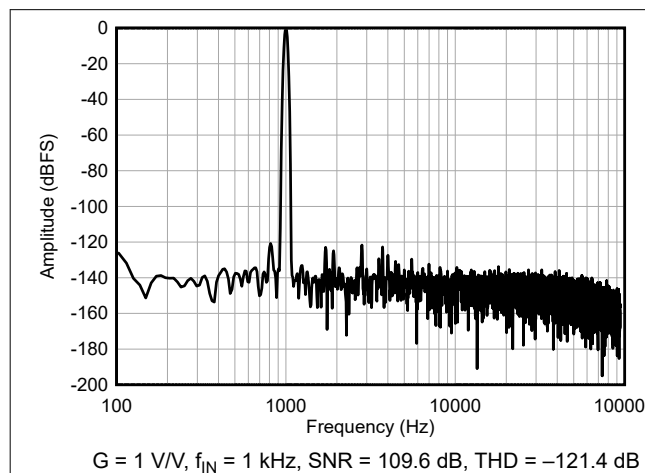


Figure 9-7. Performance FFT Plots With ADS127L11, OSR = 64, Sinc4 Filter

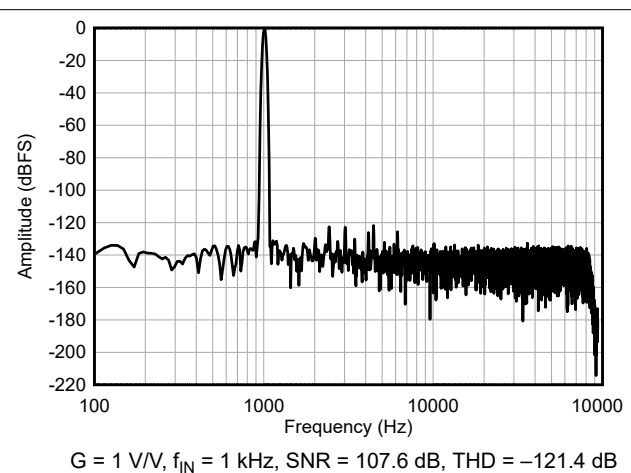


Figure 9-8. Performance FFT Plots With ADS127L11, OSR = 64, Wideband Filter

9.2.2 ADS8900B 20-Bit SAR ADC Driver Circuit

The application circuit in [Figure 9-9](#) shows the schematic for the 20-bit, precision, 1-MSPS, successive approximation register (SAR), analog-to-digital converter (ADC). This circuit is used to measure the driving capability of the PGA855 with the [ADS8900B](#) ADC. The circuit accepts single-ended or differential input signals.

The PGA855 operates with independent input and output power supplies. In this example, $\pm 15\text{-V}$ power supplies are used for the input section, and a 5.3-V power supply for the output section.

To reduce extrinsic voltage supply noise, the ADC portion of the circuit uses the [TPS7A4700](#), a low-noise, $4\text{-}\mu\text{VRMS}$ LDO voltage regulator, to generate a unipolar 5.3-V ADC supply rail and the PGA855 output stage supply is powered by the same 5.3-V ADC supply. The [REF5050](#) is selected as a voltage reference; this is a low-noise, low-drift, precision 5-V reference connected to the ADS8900B REFIN pin.

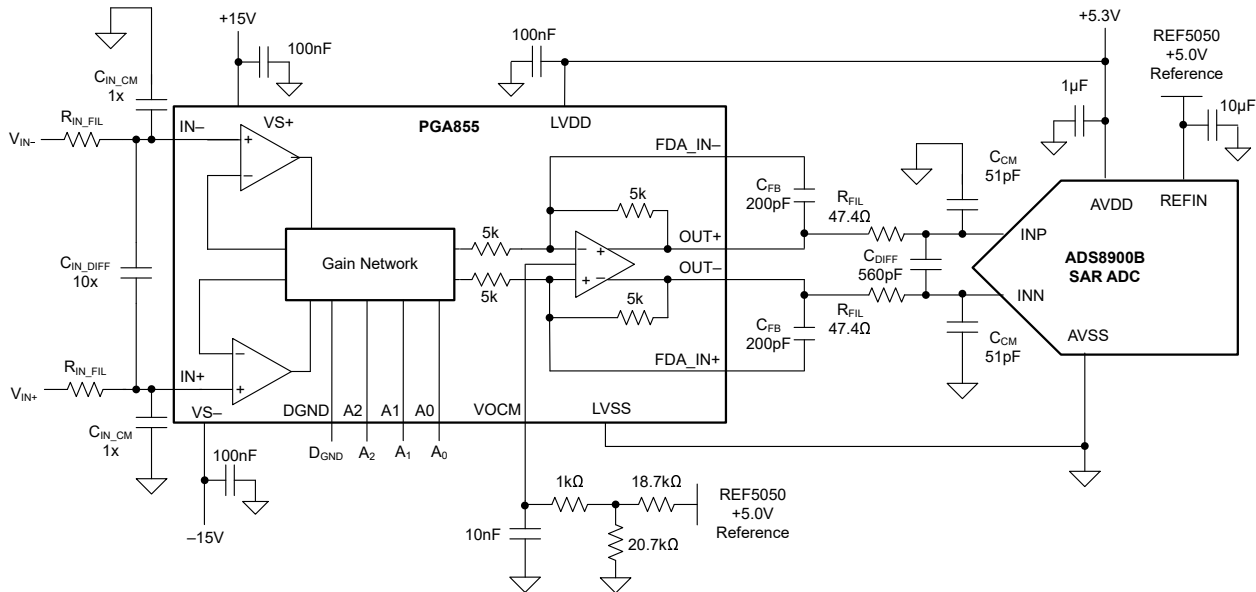


Figure 9-9. Driving the SAR ADC ADS8900B

9.2.2.1 Design Requirements

The design requirements for the application driving the ADS8900B ADC are listed in the following table.

Table 9-4. Design Parameters

PARAMETER	VALUE
Supply voltages	$V_{S\pm} = \pm 15\text{ V}$, $V_{LVDD} = 5.3\text{ V}$, $V_{LVSS} = \text{GND}$, $V_{REF} = 5\text{ V}$
Full-scale range of ADC	$\text{FSR} = \pm 5\text{ V}$
Sampling rate of ADC	$f_{\text{SAMPLE}} = 1\text{ MSPS}$
PGA gain	See Table 9-5
Input signal amplitude	See Table 9-5
Signal frequency	Tested at $f_{\text{IN}} = 1\text{ kHz}$
RC kickback filter	$R_{\text{FIL}} = 47.4\ \Omega$, $C_{\text{DIFF}} = 560\text{ pF}$, $C_{\text{CM}} = 51\text{ pF}$

9.2.2.2 Detailed Design Procedure

The ADS8900B requires an input common-mode voltage within the range of $V_{REF} / 2 \pm 100\text{ mV}$. The PGA855 V_{OCM} pin is set to a nominal voltage of approximately 2.58 V . The V_{OCM} voltage is purposely set to a voltage slightly greater than $V_{REF} / 2$ to maximize the output voltage swing range of the PGA855, while allowing margin for the V_{OCM} offset voltage error and drift variation. The V_{OCM} voltage is generated by feeding the REF5050 reference through an $18.7\text{ k}\Omega$ - to $0\text{ k}\Omega$ voltage divider implemented with 0.1% tolerance resistors. An additional RC filter with $R = 1\text{ k}\Omega$, $C = 10\text{ nF}$ is used in close proximity to the V_{OCM} pin as shown on [Figure 9-9](#).

The R-C-R differential low-pass filter at the input of the PGA helps reduce EMI/RFI high frequency extrinsic noise. This filter can be customized per the bandwidth and application requirements.

Two first-order filters are implemented with the PGA855 circuit. The first filter is provided by C_{FB} in parallel with the PGA 5-k Ω feedback resistors. The PGA resistors are $\pm 15\%$ absolute tolerance, such as, consider the effect of the tolerance on the filter cutoff frequency, the filter frequency changes to 126 kHz. At this tolerance, the filter maintains -0.1 dB flatness to 24 kHz.

There is flexibility of modifying the C_{FB} capacitor value to adjust bandwidth, with the trade-off on the broadband noise of the circuit.

The second filter placed directly at the ADS8900B inputs works as a charge reservoir to filter the sampled input of the ADC. The charge reservoir reduces the instantaneous charge demand of the amplifier, maintaining low distortion that otherwise can degrade because of incomplete amplifier settling. The RC filter combination (R_{FIL} , C_{DIFF}) is optimized for the SAR ADC sample and hold settling. This combination reduces nonlinear charge kickback of the SAR ADC and is optimized for best THD performance. This combination allows for the best trade-off between harmonic distortion while maintaining stability of the PGA output stage.

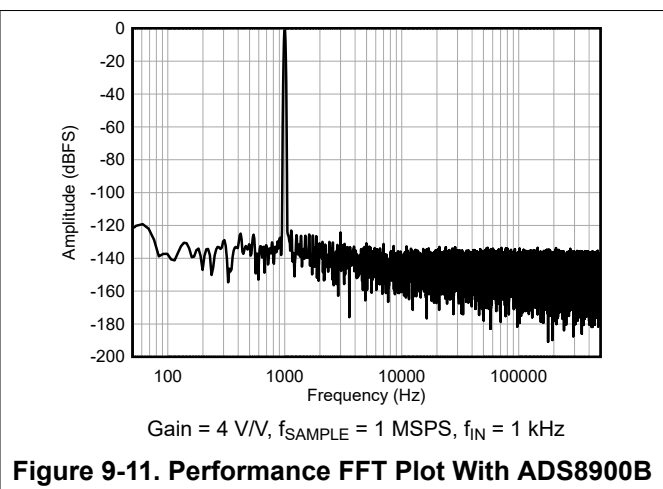
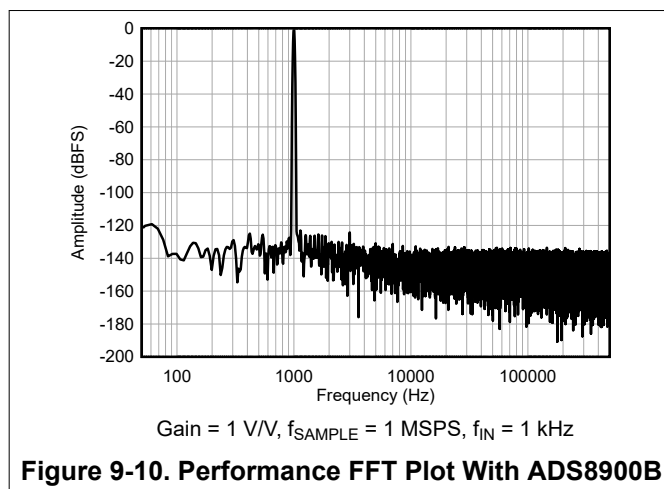
High-grade COG (NPO) are used everywhere in the signal path (C_{IN_DIFF} , C_{IN_CM} , C_{FB} , C_{DIFF} , C_{CM}) for the low distortion properties.

The results are shown in Table 9-5, which includes the typical signal-to-noise ratio (SNR) and total harmonic distortion (THD) of the PGA855 driving the ADS8900B SAR ADC. For the SNR and THD measurements, a 1-kHz differential signal is applied. The signal amplitude is adjusted to produce a PGA855 output at -0.5 dBFS of the ADC full-scale range. Table 9-5 shows the equivalent input voltage amplitude signal for different PGA855 gain configurations. At gain = 1 V/V, the design achieves a -121.4 -dB THD and 101.2-dB SNR.

Table 9-5. PGA855 and ADS8900B FFT Data Summary: $f_{SAMPLE} = 1$ MSPS, $f_{IN} = 1$ kHz

PGA GAIN (V/V)	INPUT AMPLITUDE (V _{PP})	ADC SIGNAL POWER (dBFS)	SNR (dB)	THD (dB)	ENOB (Bits)
0.125	40.10	-6.0	95.9	-118.2	15.6
0.25	36.48	-0.8	101.0	-118.6	16.5
0.5	18.24	-0.8	101.2	-121.0	16.5
1	9.12	-0.8	101.2	-121.7	16.5
2	4.56	-0.8	100.5	-121.6	16.4
4	2.28	-0.8	99.5	-121.3	16.2
8	1.14	-0.8	97.4	-119.4	15.9
16	0.58	-0.8	93.6	-117.3	15.2

9.2.2.3 Application Curves



9.3 Power Supply Recommendations

The nominal performance of the PGA855 is specified with input-stage supply and output-stage supply voltages of ± 15 V, and V_{ICM} and V_{OCM} at mid-supply. Within the specified limits, custom input and output common-mode voltages can be used without compromising performance; see also [Section 7.3](#).

CAUTION

To prevent damage to internal circuitry, the output-stage power supplies are clamped to stay within the input-stage supply voltage levels; see [Section 8.2](#).

9.4 Layout

9.4.1 Layout Guidelines

Attention to good layout practices is always recommended. For best operational performance of the device, use good PCB layout practices, including:

- To avoid converting common-mode signals into differential signals and thermal electromotive forces (EMFs), make sure that both input paths are symmetrical and well-matched for source impedance and capacitance.
- Noise can propagate into analog circuitry through the power pins of the device and of the circuit as a whole. Bypass capacitors reduce the coupled noise by providing low-impedance power sources local to the analog circuitry.
 - Connect low-ESR, 0.1- μ F ceramic bypass capacitors between each supply pin and ground, placed as close as possible to the device. A single bypass capacitor from V_{S+} and V_{LVDD} to ground is applicable for single-supply applications.
- To reduce parasitic coupling, run the input traces as far away as possible from the supply or output traces. If these traces cannot be kept separate, crossing the sensitive trace perpendicular is much better than in parallel with the noisy trace.
- Leakage on the FDA_IN+ and FDA_IN– pins can cause in a dc offset error in the output voltages. Additionally, excessive parasitic capacitance at these pins can result in decreased phase margin and affect the stability of the output stage. If these pins are not used to implement deliberate capacitive feedback, follow best practices to minimize leakage and parasitic capacitance.
- Follow best practices to minimize leakage and parasitic capacitance, which includes implementing *keep-out* areas in any ground planes that lie immediately below the input pins.
- Minimize the number of thermal junctions. If possible, route the signal path using a single layer without vias.
- Keep sufficient distance from major thermal energy sources (circuits with high power dissipation). If not possible, place the device so that the effects of the thermal energy source on the high and low sides of the differential signal path are evenly matched.
- Keep the traces as short as possible.

PGA855

SBOSAE0B – APRIL 2023 – REVISED SEPTEMBER 2023

9.4.2 Layout Example

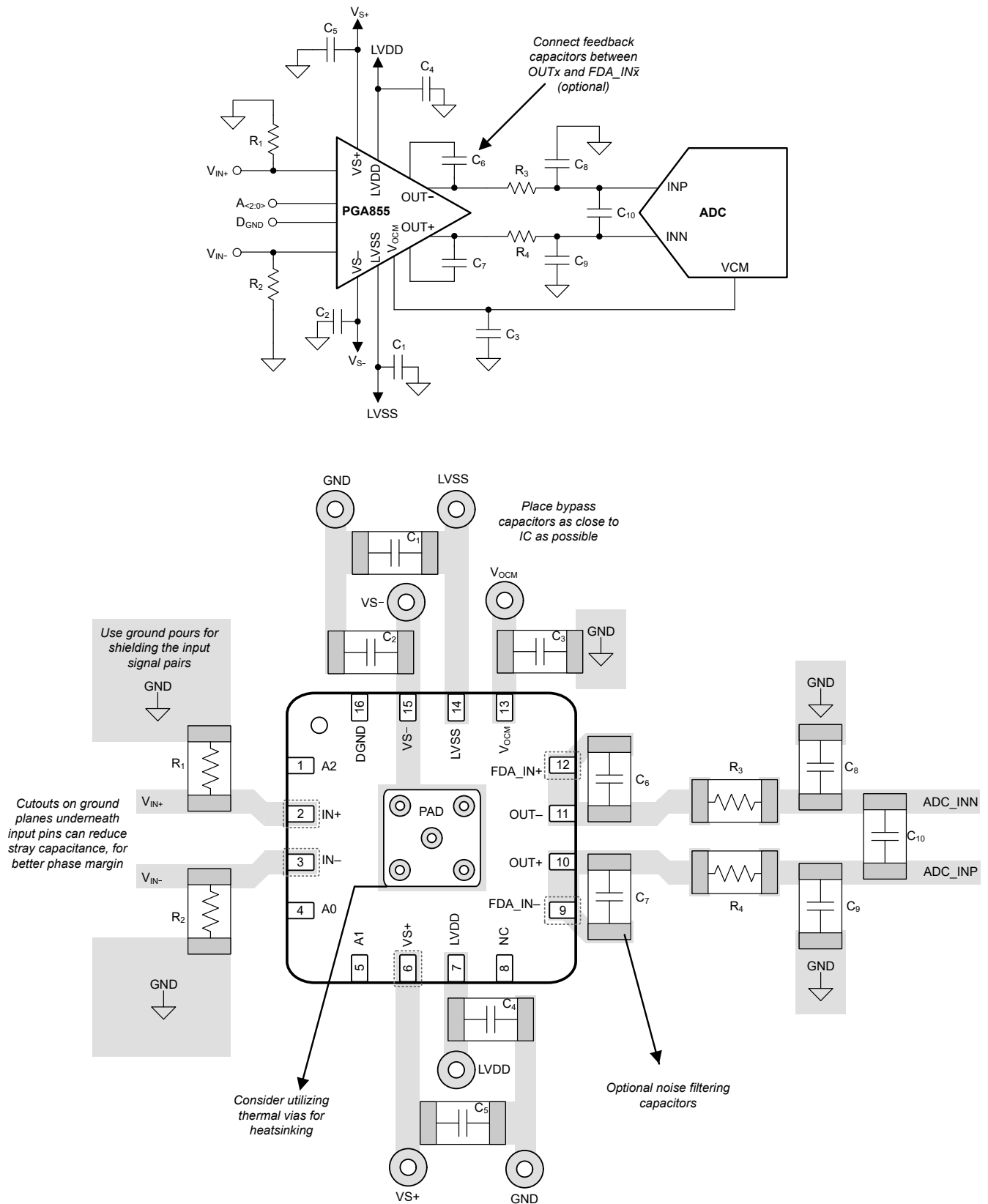


Figure 9-12. Example Schematic and Associated PCB Layout

10 Device and Documentation Support

10.1 Device Support

10.1.1 Development Support

10.1.1.1 PSpice® for TI

PSpice® for TI is a design and simulation environment that helps evaluate performance of analog circuits. Create subsystem designs and prototype solutions before committing to layout and fabrication, reducing development cost and time to market.

10.2 Documentation Support

10.2.1 Related Documentation

For related documentation see the following:

- Texas Instruments, [Comprehensive Error Calculation for Instrumentation Amplifiers application note](#)
- Texas Instruments, [Importance of Input Bias Current Return Paths in Instrumentation Amplifier Applications application note](#)

10.3 Receiving Notification of Documentation Updates

To receive notification of documentation updates, navigate to the device product folder on [ti.com](#). Click on *Subscribe to updates* to register and receive a weekly digest of any product information that has changed. For change details, review the revision history included in any revised document.

10.4 Support Resources

[TI E2E™ support forums](#) are an engineer's go-to source for fast, verified answers and design help — straight from the experts. Search existing answers or ask your own question to get the quick design help you need.

Linked content is provided "AS IS" by the respective contributors. They do not constitute TI specifications and do not necessarily reflect TI's views; see TI's [Terms of Use](#).

10.5 Trademarks

TI E2E™ is a trademark of Texas Instruments.

PSpice® is a registered trademark of Cadence Design Systems, Inc.

All trademarks are the property of their respective owners.

10.6 Electrostatic Discharge Caution



This integrated circuit can be damaged by ESD. Texas Instruments recommends that all integrated circuits be handled with appropriate precautions. Failure to observe proper handling and installation procedures can cause damage.

ESD damage can range from subtle performance degradation to complete device failure. Precision integrated circuits may be more susceptible to damage because very small parametric changes could cause the device not to meet its published specifications.

10.7 Glossary

[TI Glossary](#) This glossary lists and explains terms, acronyms, and definitions.

11 Mechanical, Packaging, and Orderable Information

The following pages include mechanical, packaging, and orderable information. This information is the most current data available for the designated devices. This data is subject to change without notice and revision of this document. For browser-based versions of this data sheet, refer to the left-hand navigation.

PACKAGING INFORMATION

Orderable part number	Status (1)	Material type (2)	Package Pins	Package qty Carrier	RoHS (3)	Lead finish/ Ball material (4)	MSL rating/ Peak reflow (5)	Op temp (°C)	Part marking (6)
PGA855RGTR	Active	Production	VQFN (RGT) 16	3000 LARGE T&R	Yes	SN	Level-1-260C-UNLIM	-40 to 125	PGA855
PGA855RGTR.B	Active	Production	VQFN (RGT) 16	3000 LARGE T&R	Yes	SN	Level-1-260C-UNLIM	-40 to 125	PGA855

(1) **Status:** For more details on status, see our [product life cycle](#).

(2) **Material type:** When designated, preproduction parts are prototypes/experimental devices, and are not yet approved or released for full production. Testing and final process, including without limitation quality assurance, reliability performance testing, and/or process qualification, may not yet be complete, and this item is subject to further changes or possible discontinuation. If available for ordering, purchases will be subject to an additional waiver at checkout, and are intended for early internal evaluation purposes only. These items are sold without warranties of any kind.

(3) **RoHS values:** Yes, No, RoHS Exempt. See the [TI RoHS Statement](#) for additional information and value definition.

(4) **Lead finish/Ball material:** Parts may have multiple material finish options. Finish options are separated by a vertical ruled line. Lead finish/Ball material values may wrap to two lines if the finish value exceeds the maximum column width.

(5) **MSL rating/Peak reflow:** The moisture sensitivity level ratings and peak solder (reflow) temperatures. In the event that a part has multiple moisture sensitivity ratings, only the lowest level per JEDEC standards is shown. Refer to the shipping label for the actual reflow temperature that will be used to mount the part to the printed circuit board.

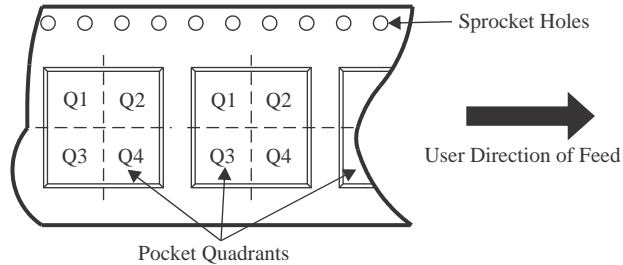
(6) **Part marking:** There may be an additional marking, which relates to the logo, the lot trace code information, or the environmental category of the part.

Multiple part markings will be inside parentheses. Only one part marking contained in parentheses and separated by a "~" will appear on a part. If a line is indented then it is a continuation of the previous line and the two combined represent the entire part marking for that device.

Important Information and Disclaimer: The information provided on this page represents TI's knowledge and belief as of the date that it is provided. TI bases its knowledge and belief on information provided by third parties, and makes no representation or warranty as to the accuracy of such information. Efforts are underway to better integrate information from third parties. TI has taken and continues to take reasonable steps to provide representative and accurate information but may not have conducted destructive testing or chemical analysis on incoming materials and chemicals. TI and TI suppliers consider certain information to be proprietary, and thus CAS numbers and other limited information may not be available for release.

In no event shall TI's liability arising out of such information exceed the total purchase price of the TI part(s) at issue in this document sold by TI to Customer on an annual basis.

TAPE AND REEL INFORMATION

QUADRANT ASSIGNMENTS FOR PIN 1 ORIENTATION IN TAPE


*All dimensions are nominal

Device	Package Type	Package Drawing	Pins	SPQ	Reel Diameter (mm)	Reel Width W1 (mm)	A0 (mm)	B0 (mm)	K0 (mm)	P1 (mm)	W (mm)	Pin1 Quadrant
PGA855RGTR	VQFN	RGT	16	3000	330.0	12.4	3.3	3.3	1.1	8.0	12.0	Q2

TAPE AND REEL BOX DIMENSIONS


*All dimensions are nominal

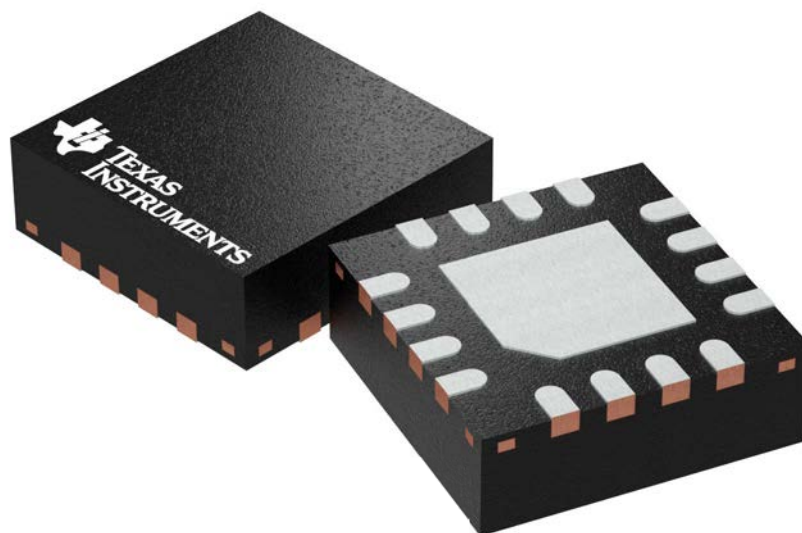
Device	Package Type	Package Drawing	Pins	SPQ	Length (mm)	Width (mm)	Height (mm)
PGA855RGTR	VQFN	RGT	16	3000	367.0	367.0	35.0

RGT 16

GENERIC PACKAGE VIEW

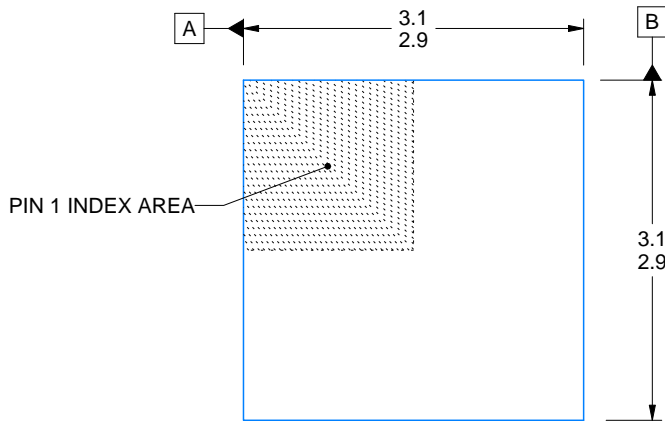
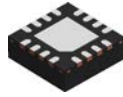
VQFN - 1 mm max height

PLASTIC QUAD FLATPACK - NO LEAD

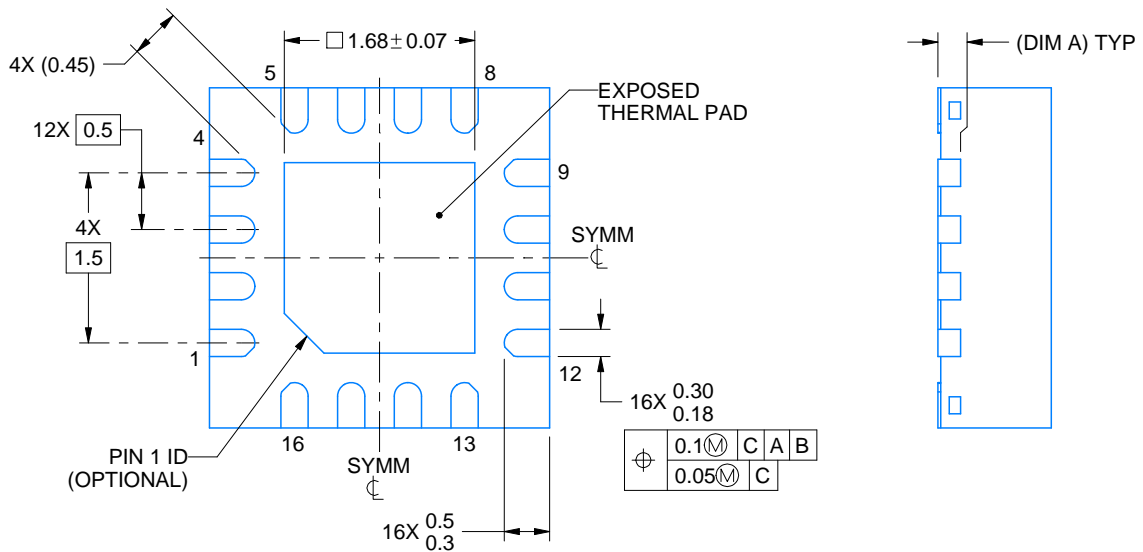
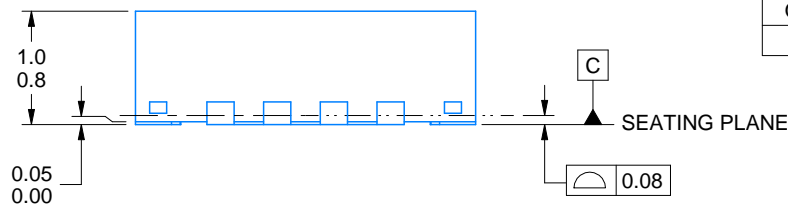


Images above are just a representation of the package family, actual package may vary.
Refer to the product data sheet for package details.

4203495/1



SIDE WALL METAL THICKNESS DIM A	
OPTION 1	OPTION 2
0.1	0.2



4222419/E 07/2025

NOTES:

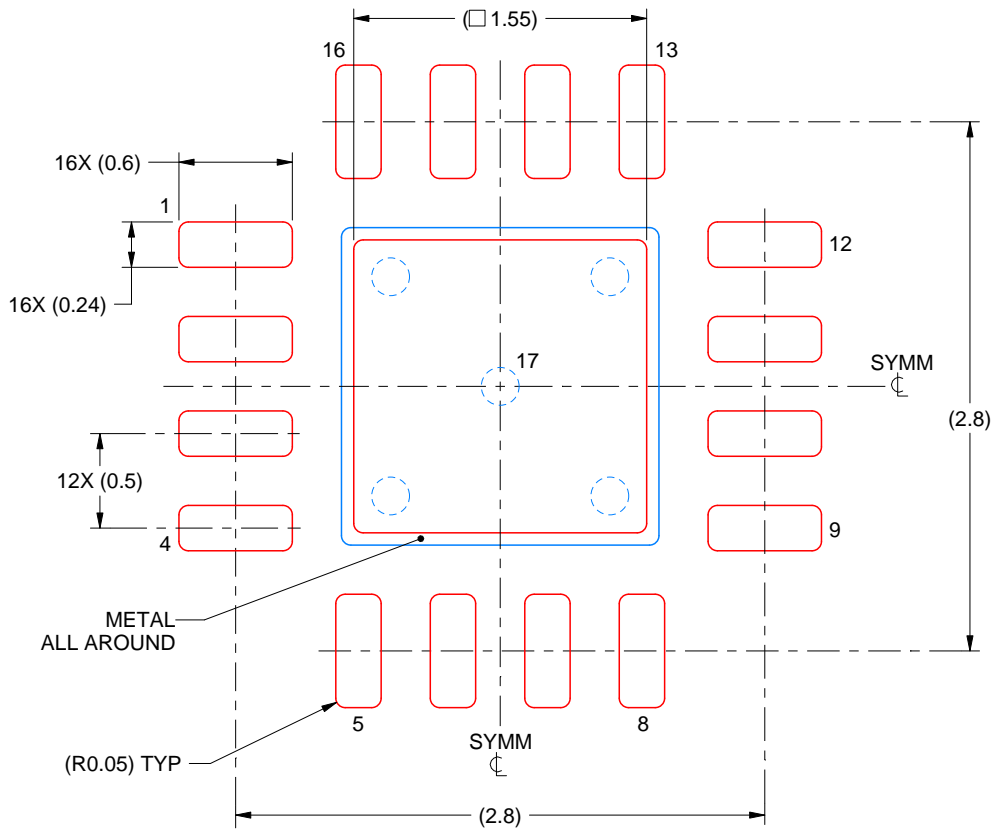
1. All linear dimensions are in millimeters. Any dimensions in parenthesis are for reference only. Dimensioning and tolerancing per ASME Y14.5M.
2. This drawing is subject to change without notice.
3. The package thermal pad must be soldered to the printed circuit board for thermal and mechanical performance.

EXAMPLE STENCIL DESIGN

RGT0016C

VQFN - 1 mm max height

PLASTIC QUAD FLATPACK - NO LEAD



SOLDER PASTE EXAMPLE
BASED ON 0.125 mm THICK STENCIL

EXPOSED PAD 17:
85% PRINTED SOLDER COVERAGE BY AREA UNDER PACKAGE
SCALE:25X

4222419/E 07/2025

NOTES: (continued)

6. Laser cutting apertures with trapezoidal walls and rounded corners may offer better paste release. IPC-7525 may have alternate design recommendations.

IMPORTANT NOTICE AND DISCLAIMER

TI PROVIDES TECHNICAL AND RELIABILITY DATA (INCLUDING DATASHEETS), DESIGN RESOURCES (INCLUDING REFERENCE DESIGNS), APPLICATION OR OTHER DESIGN ADVICE, WEB TOOLS, SAFETY INFORMATION, AND OTHER RESOURCES "AS IS" AND WITH ALL FAULTS, AND DISCLAIMS ALL WARRANTIES, EXPRESS AND IMPLIED, INCLUDING WITHOUT LIMITATION ANY IMPLIED WARRANTIES OF MERCHANTABILITY, FITNESS FOR A PARTICULAR PURPOSE OR NON-INFRINGEMENT OF THIRD PARTY INTELLECTUAL PROPERTY RIGHTS.

These resources are intended for skilled developers designing with TI products. You are solely responsible for (1) selecting the appropriate TI products for your application, (2) designing, validating and testing your application, and (3) ensuring your application meets applicable standards, and any other safety, security, regulatory or other requirements.

These resources are subject to change without notice. TI grants you permission to use these resources only for development of an application that uses the TI products described in the resource. Other reproduction and display of these resources is prohibited. No license is granted to any other TI intellectual property right or to any third party intellectual property right. TI disclaims responsibility for, and you fully indemnify TI and its representatives against any claims, damages, costs, losses, and liabilities arising out of your use of these resources.

TI's products are provided subject to [TI's Terms of Sale](#), [TI's General Quality Guidelines](#), or other applicable terms available either on ti.com or provided in conjunction with such TI products. TI's provision of these resources does not expand or otherwise alter TI's applicable warranties or warranty disclaimers for TI products. Unless TI explicitly designates a product as custom or customer-specified, TI products are standard, catalog, general purpose devices.

TI objects to and rejects any additional or different terms you may propose.

Copyright © 2026, Texas Instruments Incorporated

Last updated 10/2025

Looking for pricing, stock, or lifecycle information?

Click below to explore more details on WIN SOURCE:

 [View PIC18F16Q40-I/SS on WIN SOURCE](#)

 [Microchip Technology](#) Information

Optimize Your Supply Chain with WIN SOURCE Solutions

-  Global Sourcing Solution
-  Obsolete Management
-  Cost Control Management
-  Shortage Management
-  Alternative Solution
-  Excess Inventory Management